PREDICTION OF GRINDING MACHINABILITY WHEN GRIND P20 TOOL STEEL USING TiO_2 NANOFLUID

LAI WOON SHYZ

Report submitted in partial fulfilment of the requirements for the award of the degree of Bachelor of Mechanical Engineering with Manufacturing Engineering

Faculty of Mechanical Engineering
UNIVERSITI MALAYSIA PAHANG

JUNE 2012

UNIVERSITI MALAYSIA PAHANG

FACULTY OF MECHANICAL ENGINEERING

I certify that the project entitled "Prediction of Grinding Machinability when Grind P20 Tool Steel using TiO_2 Nanofluid" is written by Lai Woon Shyz. I have examined the final copy of this project and in my opinion; it is fully adequate in terms of scope and quality for the award of the degree of Bachelor of Engineering. I herewith recommend that it be accepted in partial fulfilment of the requirements for the degree of Bachelor of Mechanical Engineering with Manufacturing Engineering.

MR. JASRI BIN MOHAMAD
Examiner Signature

SUPERVISOR'S DECLARATION

I hereby declare that I have checked this project and in my opinion, this project is satisfactory in terms of scope and quality for the award of the degree of Bachelor of Mechanical Engineering with Manufacturing Engineering.

Signature : **……**
Name of Supervisor : DR. KUMARAN KADIRGAMA
Position : HEAD OF BIOMECHANICAL
Date : **……**

STUDENT'S DECLARATION

I hereby declare that the work in this project is my own except for quotations and summaries which have been duly acknowledged. The project has not been accepted for any degree and is not concurrently submitted for award of other degree.

Signature : **……**
Name : LAI WOON SHYZ
ID Number : ME08048
Date : **……**

Specially dedicated to

My beloved family and those who have guided and inspired me

Throughout my journey of learning

ACKNOWLEDGEMENTS

First and foremost, the deepest sense of gratitude to the God, who guide and gave me the strength and ability to complete this final year project successfully. Infinite thanks I brace upon Him. I would like to express my sincere gratitude to my supervisor Dr. Kumaran Kadirgama for his continuous guidance, support and encouragement, which gave me huge inspiration in accomplishing this research. I also sincerely thanks for the time spent proofreading and correcting my many mistakes. His practice of professional ethics encourages me to become confident and competent person to work individually as well as in group.

Besides that, I also took this opportunity to thank Mr. Aziha who helped me a lot in my experiment. He is also very supportive in exploring the features and utilization of grinding machine. A sincere appreciation to Mr. Zulfahmi, UMP Central Lab instructor who help me a lot in using Scanning Electron Microscope.

Other than that, Mr. Jasri Bin Mohamad, who reviewed and certified that my thesis is fully adequate in terms of scope and quality for the award of the degree of Bachelor of Engineering. Not forgot to thank the panels who critics the outcome of this research besides providing some suggestions to improve the discussion and conclusion as well.

I would also like to express my deepest appreciation to my family whom always support and motivate me to complete this research and thesis. I also owe a depth of gratitude to my university friends who shared their knowledge and ideas that lead to the completion of this thesis.

Finally, to individuals who has involved neither directly nor indirectly in succession of this research with thesis writing. Indeed I could never adequately express my indebtedness to all of them. Hope all of them stay continue support me and give confidence in my efforts in future.

ABSTRACT

The surface roughness is a variable often used to describe the quality of ground surfaces as well as to evaluate the competitiveness of the overall grinding system. A grinding process was performed on the P20 tool steel by changing the grinding conditions, including the depth of cut, the grinding passes, the type of wheel, and the cutting fluid supply in the experiment. The main objective of the study is to investigate the effect of TiO_2 nanofluid on the grinding surface finish and wheel tool life. The 0.1 % volume concentration of the TiO_2 nanofluid is prepared as to compare the effectiveness with the water based coolant. The selected specimens undergo SEM to assess the surface integrity of the machined surfaces. ANN prediction models are developed from the collected data.The result showed the reduction of 20 % to 40 % surface roughness value in grinding with TiO_2 nanofluid. As conclusion, TiO_2 nanofluid exhibits the better grinding surface quality. For recommendation, various machining can be conducted using nanofluid to emphasize better results.

ABSTRAK

Kekasaran permukaan adalah pembolehubah yang sering digunakan untuk menggambarkan kualiti permukaan pengisaran serta menilai daya saing keseluruhan sistem pengisaran. Satu proses pengisaran dilakukan ke atas P20 tool steel dengan menukar syarat-syarat pengisaran, termasuk kedalaman potongan, pas pengisaran, jenis roda, dan bekalan bendalir pemotongan dalam eksperimen. Objektif utama kajian ini adalah untuk mengkaji kesan TiO_2 nanofluid pada kualiti permukaan pengisaran dan hayat roda pengisaran. 0.1% kepekatan TiO_2 nanofluid disediakan untuk membandingkan keberkesanan dengan water based coolant. Enam Spesimen dipilih menjalani SEM untuk menilai integriti permukaan pemesinan. Model ramalan ANN dihasilkan dari data yang dikumpul. Keputusan eksperimen menunjukkan pengurangan 20% kepada 40% nilai kekasaran permukaan dalam penggunaan TiO_2 nanofluid. Sebagai kesimpulan, TiO_2 nanofluid mempamerkan pengisaran permukaan yang berkualiti. Percadangan selanjutnya adalah penggunaan nanofluid boleh dijalankan dalam pelbagai pemesinan untuk menekankan keputusan yang lebih baik.

TABLE OF CONTENTS

LIST OF TABLES

LIST OF FIGURES

LIST OF SYMBOLS

F_n	Normal grinding force
F_t	Tangential grinding force
Ra	Arithmetic average surface roughness
rpm	Revolution per minute
wt%	Weight percentage
V	Volume
v_s	Work table speed
v_w	Grinding wheel speed
%	Percentage
φ	Weight percentage
ρ	Density in kg/m^3
$\emptyset$	Volume percentage

LIST OF ABBREVIATIONS

AISI	American Iron and Steel Institute
Al_2O_3	Aluminium Oxide
ANN	Artificial Neural Network
C	Carbon
CNTs	Carbon Nanotubes
Cr	Chromium
Cu	Copper
DOC	Depth of Cut
Exp.	Experimental
EVO	Evolution
Fe	Iron
Mn	Manganese
Mo	Molybdenum
MSE	Mean Square Error
MQL	Minimum Quantity Lubricant
Ni	Nickel
P	Phosphorus
S	Sulphur
SEM	Scanning Electron Microscopy
Si	Silicon
SiC	Silicon Carbide
SiO_2	Silicon Dioxide
TiO_2	Anatase or Titanium Dioxide

TRN	Training
TST	Testing
VLD	Validation
UMP	University Malaysia Pahang

CHAPTER 1

INTRODUCTION

1.1 PROJECT BACKGROUND

Grinding is a material removal and surface generation process used to shape and finish components made of metals and other materials. It is one of the abrasive machining that always to achieve high enough dimensional accuracy and/or good quality surface finishes. Grinding is a manufacturing process with unsteady process behaviour, whose complex characteristics determine the technological output and quality. The quality of the surface generated by grinding determines many work piece characteristics such as the minimum tolerances, the lubrication effectiveness and the component life, among others. The grinding parameters can help to improve the wheel life and the quality of the work piece. The suitable grinding parameters can save cost, time, energy and get the good quality for surface condition. (Aguair et al., 2008)

In the past few decades, rapid advances in nanotechnology have led to emerging of new generation of coolants called “nanofluids”. Nanofluids are dilute suspensions of functionalized nanoparticles composite materials developed about a decade ago with the specific aim of increasing the thermal conductivity of heat transfer fluids, which have now evolved into a promising nanotechnological area. The enhanced thermal behaviour of nanofluids could provide a basis for an enormous innovation for heat transfer intensification, which is of major importance to grinding process as higher stock removal rates, higher quality, and longer wheel life are sought.

1.2 PROBLEMS STATEMENT

Tool steel refers to a variety of carbon and alloy steels that are particularly well-suited to be made into tools for cutting, forming, or other types of metal-working applications. Tool steels are often subjected to surface grinding. The wide differences in composition among tool steels give rise to wide variations in grinding characteristics. The P20, kind of low carbon tool steel containing chromium and molybdenum alloying elements, to fill the requirements for the machined cavities and forces used in zinc die casting and plastic molding. Hence the grinding of P20 tool steel requires high quality of surface finish. The optimum grinding parameters are crucial in pursuit of better surface finish.

Grinding process requires high energy expenditure per unit volume of material removed. Virtually all of this energy is dissipated as heat at the grinding zone where the wheel interacts with the work piece. This leads to the generation of high temperatures which can cause various types of thermal damage to the work piece. Thermal damage is one of the main factors which affects work piece quality and limits the production rates which can be achieved by grinding. Therefore, cooling and lubrication play a decisive role in grinding as to enhance process stability, better work piece quality and tool life.

1.3 PROJECT OBJECTIVES

The objective of the study is to determine the effect of TiO_2 nanofluid on the grinding surface finish and wheel wear. Secondly, is to determine the effect of the variation axial depth on the grinding surface quality. Moreover, is to investigate the influence of the grinding passes to the surface quality. Lastly, the objective is to develop artificial intelligence models using Neural Networks.

1.4 PROJECT SCOPES

The work piece used for the study is AISI P20 tool steel. The total number of grinding experiments is 54 sets of experiment. There will be 36 set experiments for grinding using water based coolant and the remains is using TiO_2 nanofluid as cutting fluid. The conducted grinding process will be single pass and multi passes grinding. The multi passes grinding is set to be 4 passes. The grinding wheel for the experiment will be Al_2O_3 grinding wheel and SiC grinding wheel. The only manipulated grinding parameter is depth of cut. The range of depth of cut is within 5 µm to 21 µm. The work table speed, v_s and grinding wheel speed, v_w are held constant throughout the experiments which are 20 m/min and 2850 rpm respectively. The water based coolant use comprises the composition of ethylene glycol and water with ratio of 6:4. The wheel and dressing conditions used for the model calibration and validation are the same for each experiment. The effect of concentration of the nanofluid is not considered in the study. Batch back propagation is used for Artificial Neural Network modelling training algorithm.

1.5 THESIS OUTLINED

This thesis consists of 5 chapters which illustrate the system design of the project. Every chapter presented with different contents. After viewing the entire chapter in the thesis hopefully viewer may conceive the system design of the project.

Chapter 1 contains of the project background, the problem statement of the project, the objectives of the project, the scopes of the project and the outline of the thesis for every chapter.

Chapter 2 contains all the literature review. This chapter will explain the information about the article that related to the project that is done by other research. This chapter also describes the journals and others important information regarding this project.

Chapter 3 is chapter for the methodology of the project. This chapter will explain about the detail of the project. It's also includes the project progress presented in flow chart and also the explanation in detail about the project.

Chapter 4 discusses the result and the analysis for this project. This chapter will explain on the results and analysis of the project. The analysis includes the comparable results between grinding experiments using water based coolant and nanofluid. Both values will be compared to justify the theory. The Artificial Neural Networks modelling prediction models of the grinding experiments are discussed.

Chapter 5 will explain the conclusion of the project. It's also includes the future recommendation of the project.

CHAPTER 2

LITERATURE REVIEW

2.1 INTRODUCTION

In this chapter, the finding and previous study regarding grinding machinability were reviewed. This chapter will present about the influence of grinding parameter on the surface quality and the tool wear. On the other hand, some concept which related to the grinding included the mechanics of chip formation and during grinding and grinding thermal effect also will be discussed in this chapter. The significant of the cutting fluid also included in the chapter. The introduction and cooling application of nanofluid are elucidating in the chapter. Besides that, this chapter also will explain about the history background and presentation of the earlier work undertaken of this study. By referring to the history background and presentation of the earlier work undertaken of this study, the expected output can be predicted. The expected output based on the previous study can be used in the result and discussion in order to justify or compared the result obtained.

2.2 GRINDING

Grinding is the finishing machining operation to ensure the final surface quality. During the grinding process, small chips are removed along with high rates of material removal. Since grinding is mostly used as finishing method, which determines the functional properties of the surface, the knowledge of the surface quality and its control are crucial. It is therefore an effort to achieve high levels of surface quality, conditionally improved by the grinding process, choosing the appropriate cutting conditions.

The quality of grinded surface is generally defined as the sum of the properties under consideration upon demands. The resulting surface quality depends on input factors such as principally cutting conditions are, followed by grinding material and accompanying phenomena. Surface quality includes physical, chemical and geometric properties. The geometric surface properties include roughness parameters as a characteristic of micro geometry in the cut plane perpendicular to the surface. (Samek et al., 2011)

2.2.1 Surface Grinding

Surface-grinding processes are classified in Germany according to DIN 8589-11 in terms of the predominantly active grinding wheel surface position and of the table feed motion type. In the case of peripheral grinding, the grinding spindle is parallel to the work piece surface to be machined. The work piece material is mainly cut with the circumferential surface of the grinding wheel.

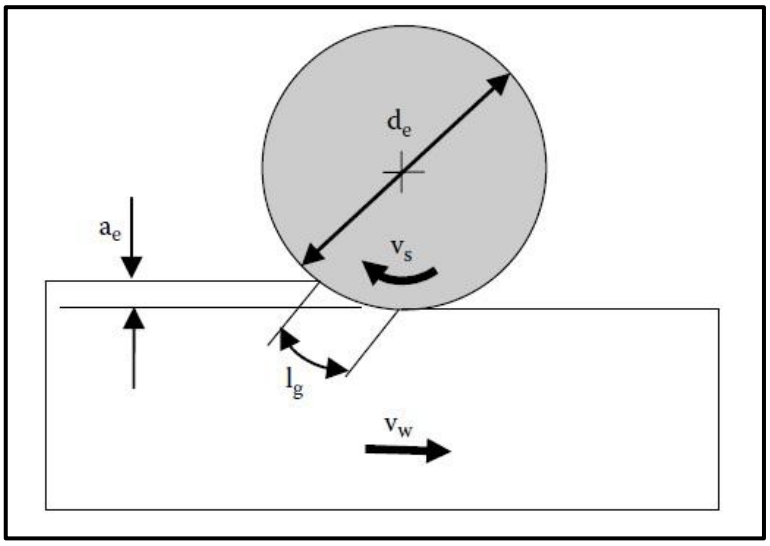

Figure 2.1: Wheel speed, work speed, depth of cut, equivalent grinding wheel diameter, and geometric contact length in grinding

Source: Marinescu et al. (2007)

2.2.2 Real Depth of Cut

The real depth of cut, a_e is the feed relative to the work piece surface. It is important to recognize that the real depth of cut is not the same as the set depth of cut. This is due to deflections of the grinding wheel, of the machine, and due to wheel wear. Grinding performance should always be related to the real depth of cut, otherwise the results will depend very strongly on the particular grinding wheel and the particular grinding machine setup.

2.2.3 Surface Roughness

Every machining operation leaves characteristic evidence on the machined surface. The quality of machined surface is characteristics by the accuracy of manufacture with respect to the dimensions specified by the designer. Surface roughness is a variable often used to describe the quality of ground surfaces and also to evaluate the competitiveness of the overall grinding system. Surface roughness is one of the most important features of a machining process because it affects the functions of the part. In a grinding process, it is very important to keep the surface roughness within specified requirements because this process is the final machining process which usually at the last stage of the machining. (Agarwal and Rao, 2007)

According to Marinescu et al. (2006), the ability of manufacturing operation is based on many factors. The final surface depends on the rotational speed of the wheel, work speed, feed rate, types of work piece being machined, depth of cut, diameter of work piece, types of wheel, and others parameter that can effect to the surface finish of the work piece. Type and amounts of lubricant use for grinding process also influence the surface roughness. Different types of machine have different variable parameters that can be change to get the best surface finish. Kalpakjian and Schmid (2006) explain about regardless of the method of the production, all surfaces have their own characteristics which collectively are referred to as surface structure. As a geometrical property is complex, certain guide lines have been established for texture in terms of well-defined and measurable quantities.

On this study, the surface roughness of the grounded area of the work piece is measured by *Ra* roughness. *Ra* roughness is the arithmetic average of all profile ordinates from a mean line within a sampling length after filtering out form deviations. (Marinescu et al., 2006)

The magnitude of the roughness is influenced by the hardness of the material ground as well as the elastic properties of the work piece, grit and binder materials. The elastic deflection of the grit at contact is generally found to be small. A grinding wheel has roughness in the axial and circumferential directions. The grinding grits flake, chip and fracture as well as is pulled out of the binder. Furthermore, when materials lying to high adhesion are ground the grit is capped by adherent lumps. The roughness of the wheel therefore changes continuously with the length and the number of passes.

2.2.4 Grinding Force

Grinding force is one of the most important parameters in evaluating the whole process of grinding. Generally, the grinding force is resolved into three component forces, namely, normal grinding force *F*n, tangential grinding force *F*t and a component force acting along the direction of longitudinal feed which is usually neglected because of its insignificance. The normal grinding force *F*n has an influence upon the surface deformation and roughness of the work piece, while the tangential grinding force *F*t mainly affects the power consumption and service life of the grinding wheel. The force plays an important role in grinding process since it is an important quantitative indicator to characterize the mode of material removal (the specific grinding energy and the surface damage are strongly dependent on the grinding force). (Agarwal and Rao, 2007)

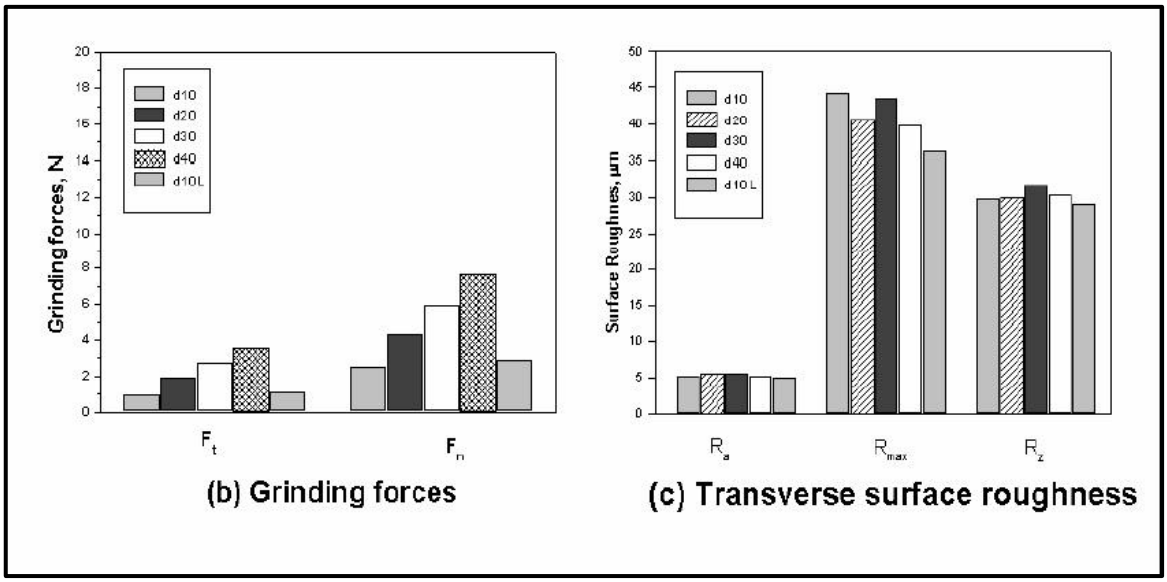

Figure 2.2: (b) Grinding forces vs depth of cut; (c)Transverse surface roughness vs depth of cut

Source: Agarwal and Rao (2007)

Grinding parameters like grinding velocity, traverse speed or wheel depth of cut affects the grinding force which in turn can cause fracture, rounding or flattening on few overlying grits thus, bringing more number of underlying grits into action. This change in topographical feature of single layer wheel, in various levels, affects the surface roughness of the work piece. Grinding force increases with decrease in grinding velocity while the same increases with increase in table speed and depth of cut. Accordingly a trend is observed on decrease of surface roughness with decrease in grinding velocity and increase of both traverse speed and wheel depth of cut.

Grinding forces not only affect chip formation mechanics, grain wear and temperature distribution but also efficiency of the grinding operation. Therefore, grinding forces are among the most important factors affecting grinding quality. (Demir et al., 2010)

2.3 MECHANICS OF CHIP FORMATION DURING GRINDING

For grinding of a work piece surface, ideal cutting can be obtained by many process combinations like ploughing due to lateral displacement, work piece movement, grinding wheel movement, elasticity of the work piece and vibration. (Midha et al., 1991)

Kinematic relation between grinding wheel and work piece in grinding process is applied to each grain of the grinding wheel. Some faces of grain during grinding can be illustrated the geometrical relation between a single grain and work piece. Non-deformed chip shape, tool path length of the abrasive grain (lk), maximum non deformed depth of cut (hm) and chip geometry are shown schematically in Figure 2.2.

Chip formation in grinding process can be divided into three successive stages: friction, ploughing and cutting. In up-cut grinding, grinding wheel grains rub on the work piece surface rather than cutting due to the elastic deformation of the system. This is called friction stage. And then, plastic deformation takes place as the elastic limit is exceeded between the abrasive grain and work piece. This is called ploughing stage. Work piece material flows plastically through forward and sideward ahead of the abrasive grain and forms a groove. When the work piece material cannot resist the flow stress, chip is formed. The chip formation is called cutting stage. In this chip formation stage, energy is used most efficiently. Rubbing and ploughing are inefficient, since the energy is wasted in deformation and friction with negligible contribution to material removal. Furthermore a high temperature may result, producing an excessive rate of wheel wear and the work piece surface may suffer metallurgical damage. (Chen and Rowe, 1995)

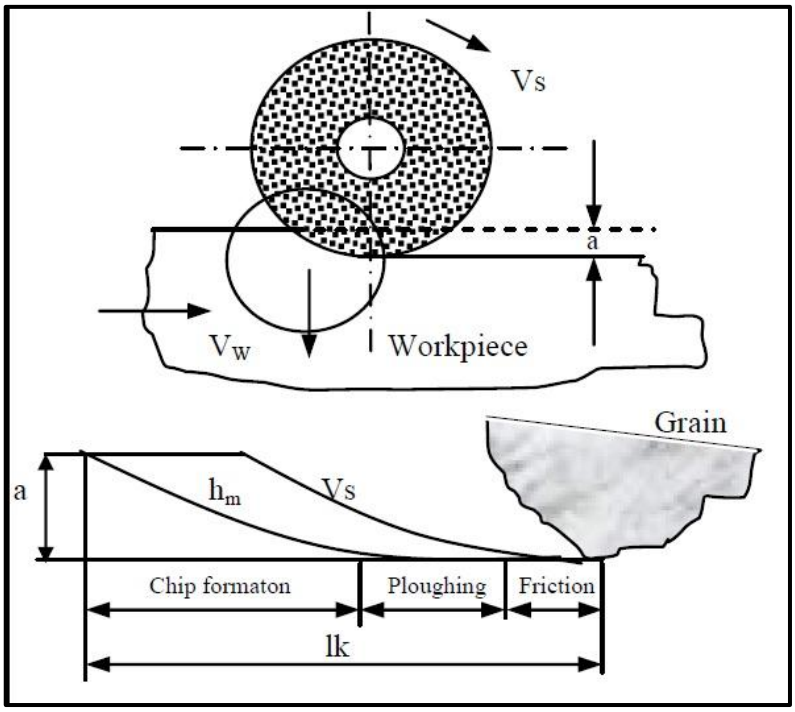

Figure 2.3: Three stages of chip generation

Source: Chen and Rowe (1995)

2.4 GRINDING THERMAL EFFECT

The grinding process requires high energy expenditure per unit volume of material removed. Virtually all of this energy is dissipated as heat at the grinding zone where the wheel interacts with the work piece. This leads to the generation of high temperatures which can cause various types of thermal damage to the work piece, such as burning, metallurgical phase transformations, softening (tempering) of the surface layer with possible re-hardening, unfavourable residual tensile stresses, cracks, and reduced fatigue strength of the work piece. Thermal damage is one of the main factors which affects work piece quality and limits the production rates which can be achieved by grinding, so it is especially important to understand the underlying factors which affect the grinding temperatures.

The temperatures are generated during grinding as a consequence of the energy expended by the process. In general, the energy or power consumption is an uncontrolled output of the grinding process. Thermal analyses of grinding processes are usually based upon the application of moving heat source theory. All the grinding energy expended is considered to be converted to heat at the grinding zone where the wheel interacts with the work piece. A critical parameter needed for calculating the temperature response is the energy partition to the work piece, which is the fraction of the total grinding energy transported to the work piece as heat at the grinding zone. The energy partition depends on the type of grinding, the wheel and work piece materials, and the operating conditions. (Malkin and Gou, 2007)

2.5 GRINDING WHEEL

In grinding wheels, the cutting edges produced by the abrasive grains are arranged in a random fashion. Randomly arranged grains produce, in turn, a surface which profile could be considered as random. Torrance and Badger (2000) detailed the study of grinding wheel surfaces and have been reported on the measurement and analysis of the working surface of grinding wheels**.** Since the grinding wheel has a high surface speed compared with the work piece surface, the surface of the grinding wheel which contributes to the cutting could well be taken as the effective profiles of the wheel comprising all the high points on the individual sections of the wheel. Attempts have been made to obtain this effective profile by superimposing individual section profiles, but it is an elaborate and time consuming approach. (Torrance and Badger, 2000)

2.5.1 Wheel Dressing

The procedures and mechanisms of dressing grinding wheels is critical to obtaining optimum performance in grinding. Truing: Creating a round wheel concentric to the axis of wheel rotation, and generating, if necessary, a particular profile on the wheel face. It is also to clean out any metal embedded or “loaded” in the wheel face. A further function is to obtain a new set of sharp cutting edges on the grains at the cutting surfaces. Conditioning: Preferential removal of bond from around the abrasive grits.

Dressing: Truing the wheel and conditioning the surface sufficient for the wheel to cut at the required performance level. (Marinescu et al. 2006)

Vickerstaff (1975) have shown that a grinding wheel produces features on the work piece surface which can be directly attributed to the wheel dressing process. The traverse rate and shape of the single-point dressing diamond are particularly important. The diamond actually cuts through the abrasive grit to produce what is effectively a form tool. The dimensions of this form are determined by the combination of diamond traverse rate, shape and in feed. When the wheel is used for grinding the abrasive grits transfer their profile to the work piece surface.

The wheel was dressed with a single-point pyramidal diamond and the debris collected on grease covered glass slide. After dissolving away the grease and the metal chips the dressing particles were sieved and weighed to determine their size distribution. The original grit size and the wheel hardness were found to influence the size distribution of the dressing particles. Generally smaller grits and harder wheels gave smaller dressing particles. More significantly however, the dressing particles for all the wheels used were not much smaller than the grits which went into the wheels, indicating that the dressing diamond actually fractures grits to' produce relatively large fragments or, possibly, dislodges them from the bond. (Vickerstaff, 1975)

2.5.2 G-Ratio

G-ratio is used as the primary measure of wheel wear. This is defined as

$$\text{G ratio} = \frac{\text{Volume of material ground per unit wheel width}}{\text{Volume of wheel worn per unit wheel width}} \qquad (1.1)$$

G-ratio is dimensionless with values that can vary from <1 for some soft alox creep feed vitrified wheels to as high as 100,000 for vitrified CBN wheels. G-ratio will fall linearly with increases in Q' accelerating to an exponential drop as the maximum metal removal rate for the wheel structure is reached. (Marinescu et al. 2006)

2.6 CUTTING FLUIDS

Cutting fluid is a term generally used to describe grinding fluids used for cooling and lubrication in grinding. The main purpose of a grinding fluid is to minimize mechanical, thermal, and chemical impact between the active partners of the abrasion process. The lubricating effect of a grinding fluid reduces friction between the abrasive grains and the work piece, as well as between the bond and the work piece. A second requirement of a grinding fluid is direct cooling of the grinding contact zone through the absorption and transportation of the heat generated in the grinding process. Other functions of a grinding fluid are the evacuation of chips from the contact zone, bulk cooling of the work piece and the grinding machine, and corrosion protection. (Marinescu et al., 2006).

Cooling and lubrication requirements differ in every application and mainly depend on grinding conditions. Coolants should, ideally, be composed to suit each specific case. Every coolant consists of a basic fluid, to which are added other products such as anti-wear, anticorrosion or emulsifying agents.

2.6.1 Effectiveness of Cutting Fluid

A cutting fluid has three main functions when applied to the grinding process. There are, bulk cooling of the work piece, the flushing away of the chips and dislodged wheel grits and lubrication. Bulk cooling and flushing are reasonably understood but the lubrication effects of the cutting fluid are less clear. It is generally accepted that cutting fluids lower the grinding zone temperature due to lubrication, which reduces wheel dulling, rather than by removing heat from the grinding zone. By reducing wheel dulling, friction and hence power is reduced so that the heat generated is limited. Bulk cooling and flushing can be achieved even though very little fluid enters the contact region between the grinding wheel and work piece. Lubrication depends on fluid entering the contact region and although a large volume may not be necessary to achieve this purpose, fluid delivery will be ineffective if no fluid enters the grinding zone. (Ebbrell et al., 1999)

2.7 NANOFLUID

Nanofluids are a relatively new class of fluids which consist of a base fluid with nano-sized particles (1–100 nm) suspended within them. These particles, generally a metal or metal oxide, increase conduction and convection coefficients, allowing for more heat transfer out of the coolant. (Serrano et al., 2009)

In earlier research has shown that the thermal conductivity and the convection heat transfer coefficient of the fluid can be largely enhanced by the suspended nanoparticles. Recently, tribology research shows that lubricating oils with nanoparticle additives exhibit improved load-carrying capacity, anti-wear and friction reduction. These features make the nanofluid very attractive in some cooling or lubricating application in many industries including manufacturing, transportation, energy, and electronics. (Shen, 2008)

Nanofluids are defined as suspension of nanoparticles in a base fluid. Nanofluids are dilute suspensions of functionalized nanoparticles composite materials developed about a decade ago with the specific aim of increasing the thermal conductivity of heat transfer fluids, which have now evolved into a promising nanotechnological area. Such thermal nanofluids for heat transfer applications represent a class of its own difference from conventional colloids for other applications. Compared to conventional solid–liquid suspensions for heat transfer intensifications, nanofluids possess the advantages such as high specific surface area and therefore more heat transfer surface between particles and fluids, reduced particle clogging as compared to conventional slurries, thus promoting system miniaturization and adjustable properties, including thermal conductivity and surface wettability, by varying particle concentrations to suit different applications.

2.7.1 Nanofluids for Cooling Application

Heat transfer fluids play an important role for cooling applications in many industries including manufacturing, transportation, energy, and electronics. According to Shen (2008), developments in new technologies such as highly integrated

microelectronic devices, higher power output engines, and reduction in applied cutting fluids continuously increase the thermal loads, which require advances in cooling capacity. Therefore, there is an urgent need for new and innovative heat transfer fluids to achieve better cooling performance. Generally, conventional heat transfer fluids have poor heat transfer properties compared to solids. Therefore, fluids containing suspended solid particles are expected to display significant enhancement in thermal conductivities relative to conventional heat transfer fluids. Numerous theoretical and experimental studies of the effective thermal conductivity of fluids containing particles have been conducted since Maxwell's theoretical work was published more than 100 years ago. However, these studies were confined to dispersions containing millimeter- or micrometer-sized particles. In developing advanced fluids for industrial applications, it was identified that millimeter or micrometer-sized sized particles have severe clogging and abrasive problems. With the development of Nano powder synthesizing techniques, it was proposed that nanometer sized solid particles can be uniformly and stably suspended in industrial heat transfer fluids such as water, ethylene glycol, or engine oil to produce a new class of engineered fluids with high thermal conductivity. (Shen, 2008)

There are major challenges in the rapid settling of these particles in fluids. The nanoparticles that suspended much longer than micro particles remain indefinite. Surface area to volume ratio is much larger in million times than micro particles. These property enhanced flow, heat transfer and other characteristics.

The behaviour of fluids at micro level is different from macro fluid in that surface tension, energy dissipation and fluidic resistance start to dominate the system. Molecular transport between them must often be through diffusion. Nanofluids are having low Reynolds number. When Reynolds number is low, the viscous interaction between wall and fluid is strong and there is no turbulence or vortices. Transport by diffusion can be very effective means of mixing in the low Reynolds number regime. Conventionally fluids have poor thermal conductivity. Conventional fluids contain mm or μm size particles do not work with miniaturized technology because they can clog the tiny channels of these devices. Nanofluids are new class of advanced heat transfer fluids engineered by dispersing nanoparticles smaller than 100 nm in diameter in conventional heat transfer fluids. (Saidur et al., 2010)

2.8 JOURNALS SYNTHESIS

2.8.1 Surface Roughness

According to Hecker and Liang (2003) the surface roughness model is based on the chip thickness model that includes many parameters such as: the wheel microstructure, the kinematic conditions, and the material properties. Therefore, the model can be used to predict the surface roughness under different conditions of these parameters. The depth of cut and the speed ratio are the two most common kinematic variables set on the machine to obtain the desired grinding outputs. Figure 2.4 shows the surface roughness versus the depth of cut for three different speed ratios. It can be observed that variations on the depth of cut, in its lower range, produce significant changes on the value of the surface roughness. The model also predicts that at higher speed ratios the surface produced is smoother. This is because at higher speed ratio that is at higher wheel velocity or lower work piece velocity, more grains participate in removing a given volume of material hence the depth of engagement is lower, producing smooth surfaces.

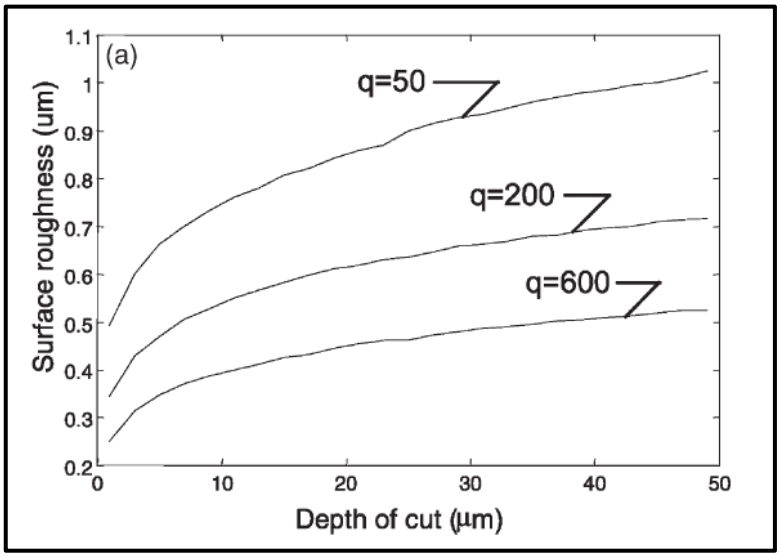

Figure 2.4: Surface roughness versus depth of cut for three different speeds

Source: Hecker and Liang (2003)

Hecker and Liang (2003) also stated that the wheel microstructure plays a major role in the quality of the ground surfaces. The wheel and dressing conditions used for the model calibration and validation were the same for each experiment. Figure 2.5 shows surface roughness for two different grinding wheels which have different hardness. As a result the finer wheel produces better surface finish but it will cause higher forces and higher power due to the higher specific energy governed by a smaller expected value of the chip thickness. (Hecker and Liang, 2003)

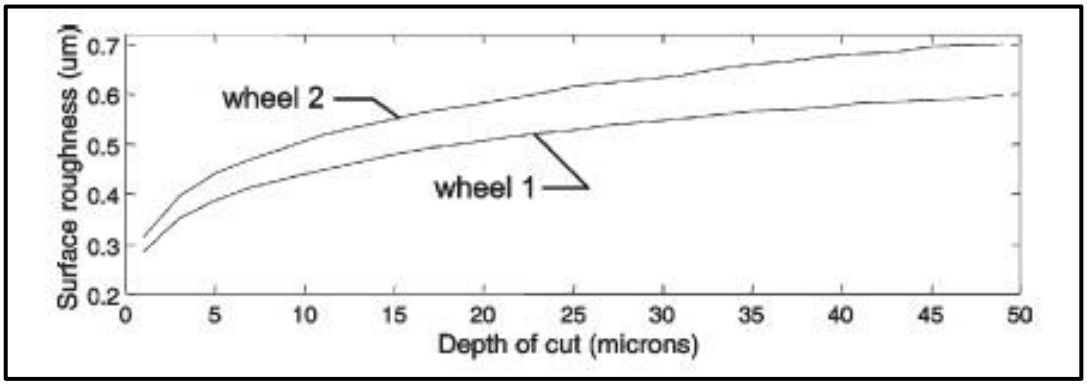

Figure 2.5: Surface roughness versus depth of cut for two different wheels

Source: Hecker and Liang (2003)

According to Shaji and Radhakrishnan (2002), the increasing of infeed or depth of cut will yield the increasing of surface roughness Ra. Figure 2.6 below show the result surface roughness vs experiment factor level. From the graph, the surface roughness increases with the increase of feed (F), infeed (IF) and coarseness of dressing (DR) and it decreases with increase of speed (S).

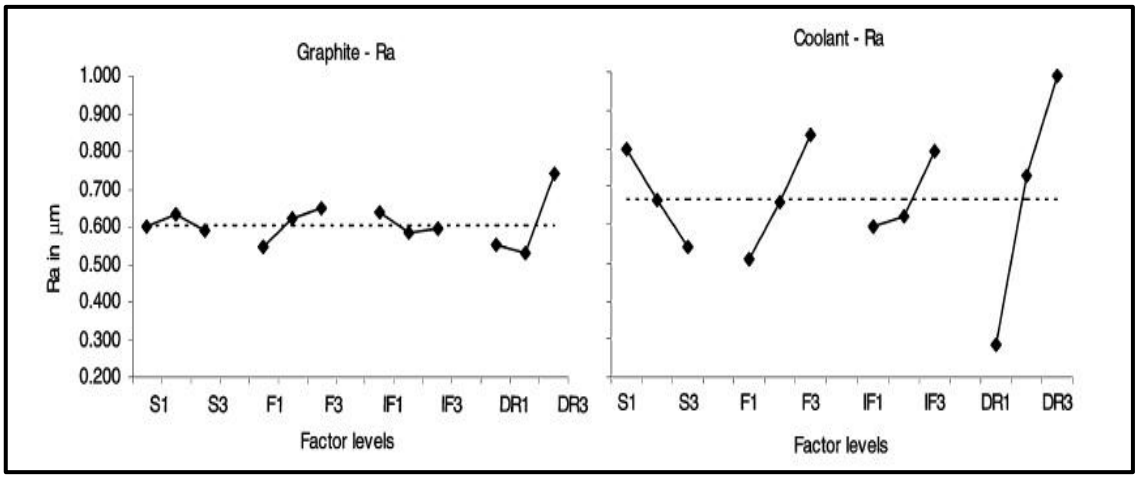

Figure 2.6: Level average response graphs for various quality characteristics in different grinding by observed data

Source: Shaji and Radhakrishnan (2002)

The tangential force component is directly proportional to the mean undeformed chip thickness, which in turn is directly proportional to the infeed. The quantity of infeed is found to be the prominent factor influencing the normal and tangential force components in both the grinding systems. As the forces developed in the process directly depend upon the undeformed chip thickness the prominent influence of infeed on forces is justified The trend in the force components in conventional grinding with respect to the fineness of dressing is reasonably understandable. Finer dressing with lower dressing lead and depth produces high density cutting edges with wider flats on the grains, which penetrate less easily into the work material causing high normal forces. In such cases, sliding and plowing components will be higher. As a result of high friction and increased amount of plastic deformation the tangential force is also higher. With coarser dressing, grits are damaged severely and the plateau area/grit will be smaller, leading to lower force components. (Shaji and Radhakrishan, 2002)

According to Samek et al. (2011), it is possible to say that to the increasing depth of cut roughness parameter increases approximately in direct proportion. The greater heat generation during the grinding, compared to the other materials, resulting in deterioration of ground surface. The results show that the increasing depth of cut has adverse effect on the surface quality. Moreover, the surface roughness measurement

was influenced by grinding grains, remained bonded on the surface, leading to difficult quantification of roughness parameters. Moreover while grinding; melted chips are adhered on the grinding wheel as well as on the surface material, which has a negative effect on surface roughness.

2.8.2 Effectiveness of Nanofluid on Grinding

According to Prabhu and Vinayagam (2011), the specimens machined using nanofluids exhibit better surface finish as compared to specimens machined without using nanofluids. Moreover a higher speed and feed will cause a poorer surface finish. The result also shows an excellent machined finish can be obtained by adding carbon nanotubes CNTs to cutting fluids and setting the machine parameters at an optimum speed and feed. The mixture of SAE20W40 oil with multiwall CNTs shows a clear increase in flash and fire point before and after the addition of nanoparticles. It shows that there is a significant improvement in thermal property. Due to increase in surface area to volume ratio of nanofluids particularly the variation of viscosity in high temperature region is less for nanofluids. The authors concluded the surface finish of work piece is elevated to nano level.

Saidura et al. (2010) stated that Heat liberated and the friction associated with the cutting process ever pose a problem in terms of tool life. Cutting fluids have been the conventional choice to address the problem. Nanofluids, with their cooling and lubricating properties, have emerged as a promising solution. Cutting fluids with inclusion of nanoparticles have enhanced heat transfer capacity up to 6%.

The grinding process generates an extremely high input of energy per unit volume of material removed. Virtually all this energy is converted to heat, which can cause high temperatures and thermal damage to the work piece such as work piece burn, phase transformations, undesirable residual tensile stresses, cracks, reduced fatigue strength, and thermal distortion and inaccuracies. The advanced heat transfer and tribological properties of these nanofluids can provide better cooling and lubricating in the MQL grinding process, and make in production-feasible.(Saidura et al., 2010)

Shen (2008) researched the wheel wear and tribological characteristics in fluid, dry and minimum quantity lubrication (MQL) grinding of cast iron. Water-based alumina and diamond nanofluids were applied in the MQL grinding process and the grinding results were compared with those of pure water. Nanofluids demonstrated the benefits of reducing grinding forces, improving surface roughness, and preventing burning of the work piece. Contrasted to dry grinding, MQL grinding with nanofluids could considerably lower the grinding temperature and exhibit the better surface finish.

2.8.3 Wheel Wear

Pande and Lal (1975) have conducted an experiment on wheel wear in dry grinding surface. The result of their study shows that the wheel wear is increase together with increasing of volume of material removal rate. They have use two method to detect the wheel wear in grinding machinability, which is from Figure 2.7 (a) measurements of wheel diameter and also from Figure 2.7 (b) abrasive grains collected from the debris. Figure 2.7 shows the graph of volume of wheel wear versus volume of material removed. The wheel wear is increased when the volume of material removed from the work piece. From the Figure 2.7, the wheel wear reduction of wheel diameter gives very high values. Figure 2.7 also shows that different wheel have different wheel wear. Wheel A46 H5 V10 (a') has higher wheel wear compared to wheel A60 J5 V10 (b').

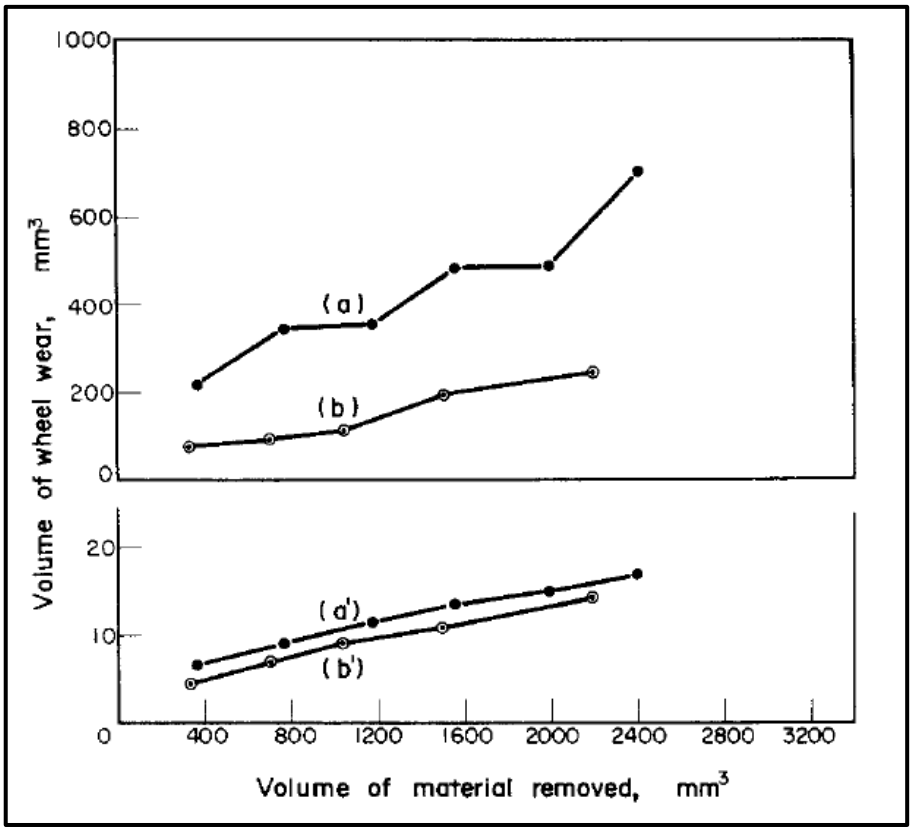

Figure 2.7: Graph volume of wheel wear versus volume of material removed

Source: Pande and Lal (1975)

Pande et al. (1979) has discussed about the variation of wheel wear and force with the number of passes. Pande et al. (1979) has shown the typical curves of variation of wheel wear and forces with the number of passes are shown in Figure 2.8 and Figure 2.9 respectively. The wheel wear was evaluated from the weight of wear particles collected during grinding. Phase I and phase II are clearly distinguishable. In phase II the wheel wear increases linearly whereas the forces remain more or less constant. Pande et al. (1979) specified that the grinding ratio can be obtained from the slope of the curve in phase II.

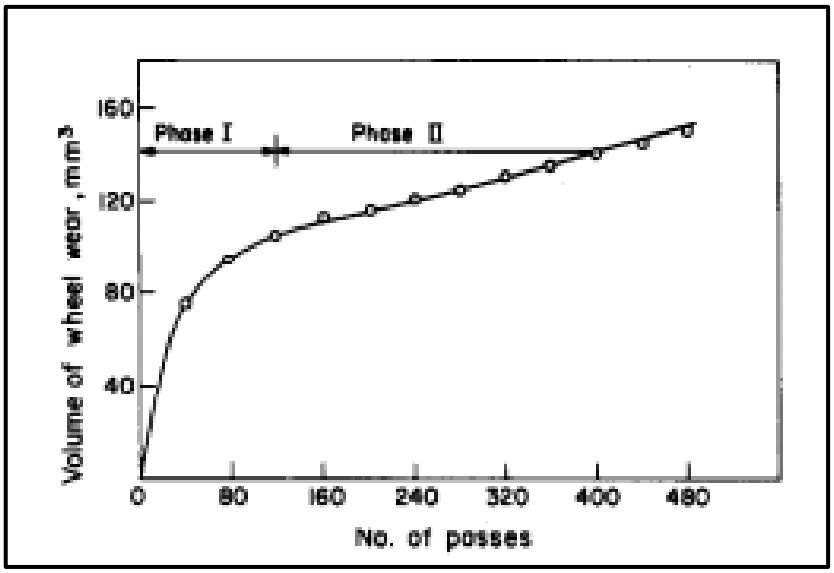

Figure 2.8: Variation of wheel wear with the number of passes

Source: Pande et al. (1979)

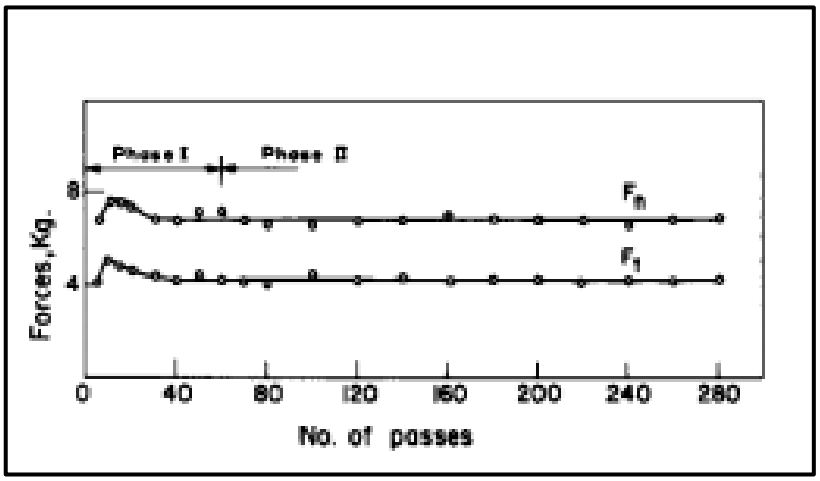

Figure 2.9: Variation of force with the number of passes

Source: Pande et al. (1979)

Pande and Lal (1975) conducted an experimental study on wheel wear on dry surface grinding. Figure 2.10 shows the experimental results which is the grinding ratio decreases with depth of cut. This indicated that the wheel wear increased with increase in depth of cut.

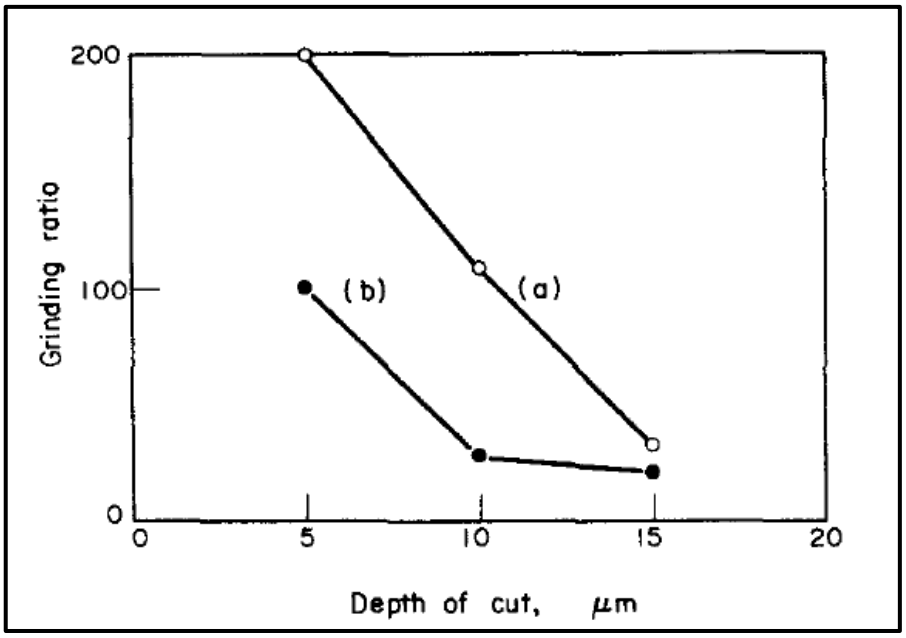

Figure 2.10: Variation of grinding ratio versus depth of cut

Source: Pande and Lal (1975)

2.8.4 Friction, Cooling and Lubrication in Grinding

Brinksmeier et al. (1999) stated that in grinding, the chip is formed, as material is deformed by the grit or grain cutting edge and displaced sideways or forward according to the orientation of the cutting edge. When the material' shear stress is exceeded, the chip flows over the face of the grain. The coolant in the contact zone influences the chip formation process by building up a lubricant film, thus lowering the friction forces, and cooling the material and tool surfaces. As the lubrication effect increases, there is a corresponding increase in elastic-plastic deformation under the cutting edge of the abrasive grain, resulting in a decrease in work piece roughness.

By reducing friction forces, friction heat is reduced and therefore also the total process heat. However, too much lubrication can have negative thermal effects, as the efficiency of the cutting process is reduced and relatively more energy is used in the shearing and deformation processes. Another important influence of coolant on lubrication is the lowering of friction along the chip flow line, i.e. between the chip, the

grain cutting edge and the grinding wheel bond. This reduces bond abrasion and grinding wheel wear. (Brinksmeier et al., 1999)

Sedlacek et al. (2008) proposed that the lubrication leads to the decrease of the wheel-work piece friction coefficient and preserving the grinding wheel sharpness, and thus reduces the cutting forces and cutting energy. Good lubrication in the grinding zone can largely reduce the sliding forces, and then the grinding force and the grinding force ratio will become lower. The good surface will be obtained as the more effective lubrication and cooling of the abrasive grains at the work piece-wheel interface. Efficient lubrication allows the chips to slide more easily over the tool surface and results in a better surface finish.

Tawakoli et al. (2010) stated that the coolant-lubricant in the grinding process influences the chip formation process by building up a lubricant film, thus lowering the friction forces, and cooling the contact zone. The cutting fluid oil with highest viscosity results in finer surface. The better surface roughness values employing low porosity and finer grains can be explained by dulling of the grits. The dull grits and a film cutting fluid between the grit wear flat area and work piece surface smooth the surface on the one hand and enlarge the deformation zone in the contact area on the other hand. A successful coolant-lubricant might be thought to form a low shear strength layer between the grain wear flat face and the work piece surface to eliminate the region of strong adhesion.

The mechanism of the abrasive grain micro wear is based on different physical-mechanical phenomena, like mechanical friction, adhesion, corrosion, diffusion and heat stress. The lower grinding forces and friction generated when using the oil in comparison with when applying water miscible cause lower mechanical loads on the bond material and abrasive grains and consequently lower wheel wear. (Tawakoli et al., 2010)

CHAPTER 3

METHODOLOGY

3.1 INTRODUCTION

This chapter discussed the research methodology and the planning stage of this project. In this study, AISI P20 tool steel of dimension (120 mm x 180 mm x 20 mm) is used as work piece to undergo the grinding experiments. The grinding experiments have been undertaken with various axial depth of cut within the range of 5 μm to 21 μm. The grinding wheels used in this study are SiC wheel and Al_2O_3 wheel. The conducted grinding process will be single pass and multi passes grinding. The surface roughness of the grounded area is measured in order to determine the relationship between the surface quality and the axial depth of cut.

The grinding experiments conducted with two different type of cutting fluid which are water based coolant and TiO_2 nanofluid. The volume concentration of the TiO_2 nanofluid is set as 0.1 %. The TiO_2 nanofluid with volume concentration of 0.1 % is prepared by single step dilute approach. The grinding experiments are then conducted using SiC wheel with single and multi passes grinding method. The surface roughness of the grounded area and the wheel wear is then measured. This enables the comparison between the effect of water based coolant and the TiO_2 nanofluid on the surface quality and the tool life. The procedure for the experiments from preparing nanofluid and measure the surface roughness and the design of experiments in this research will be discussed in details in this chapter.

The selected samples from the multi passes grinding experiments using SiC grinding wheel undergo the Scanning Electron Microscope (SEM) in order to assess the surface integrity of the machined surfaces and subsurface damage. The samples were

observed in the as-machined condition. Artificial Neural Network (ANN) is used to model the grinding surface roughness after all the result of the 54 sets grinding experiments generated. A flow chart was used to indicate the flow of the whole study was shown in Figure 3.1.

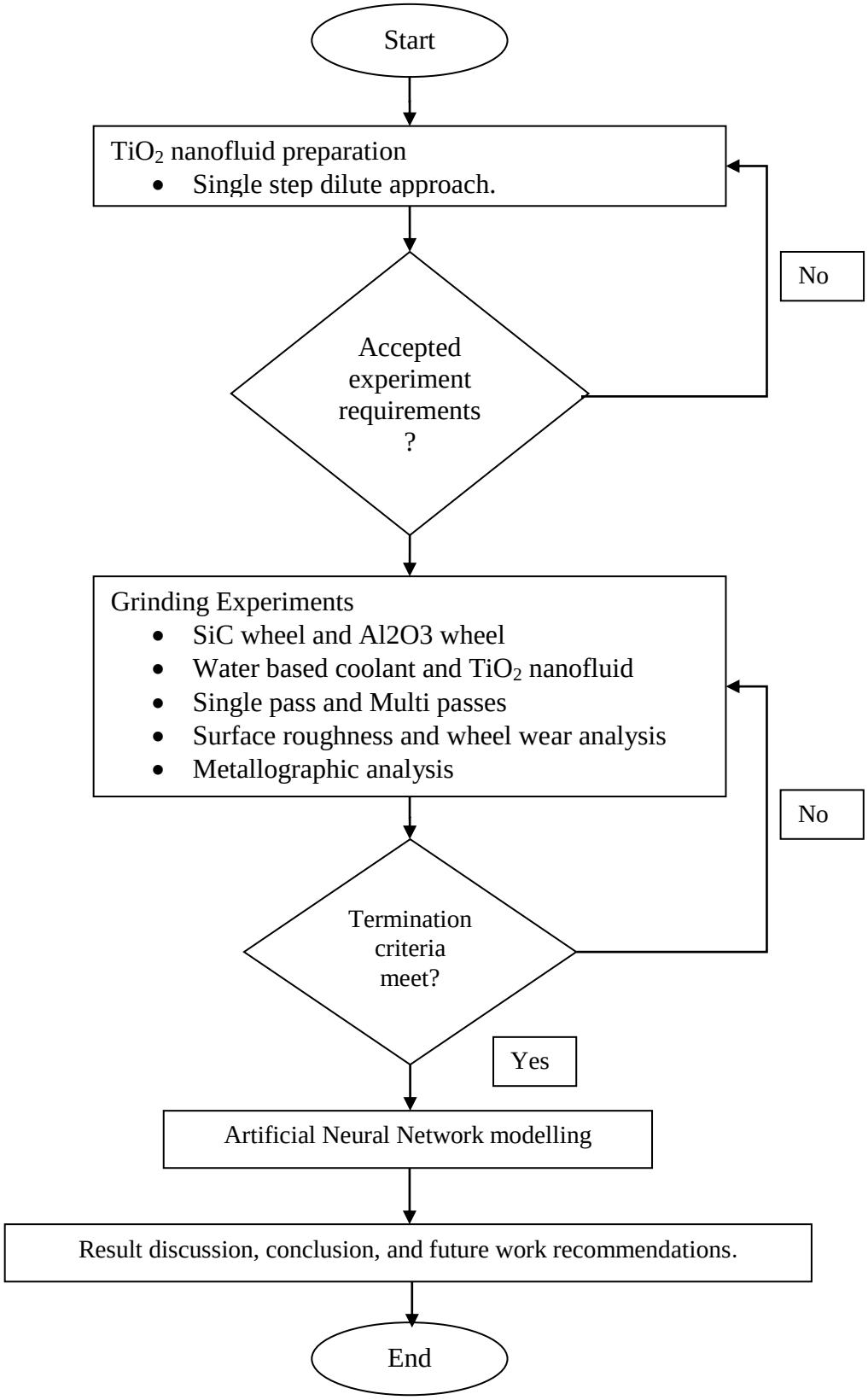

Figure 3.1: Flow chart of summarize research methodology

3.2 WORK PIECE

The work piece used to ground in the study is AISI P20 tool steel. The AISI P20 tool steel is a kind of low carbon tool steel containing chromium and molybdenum alloying elements. The hardness of the AISI P20 tool steel is approximately Brinell hardness number of 300. Figure 3.2 shows the work piece of slab structure with dimension of 120 mm x 180 mm x 20 mm. Table 3.1 shows the chemical composition of the AISI P20 tool steel (wt%).

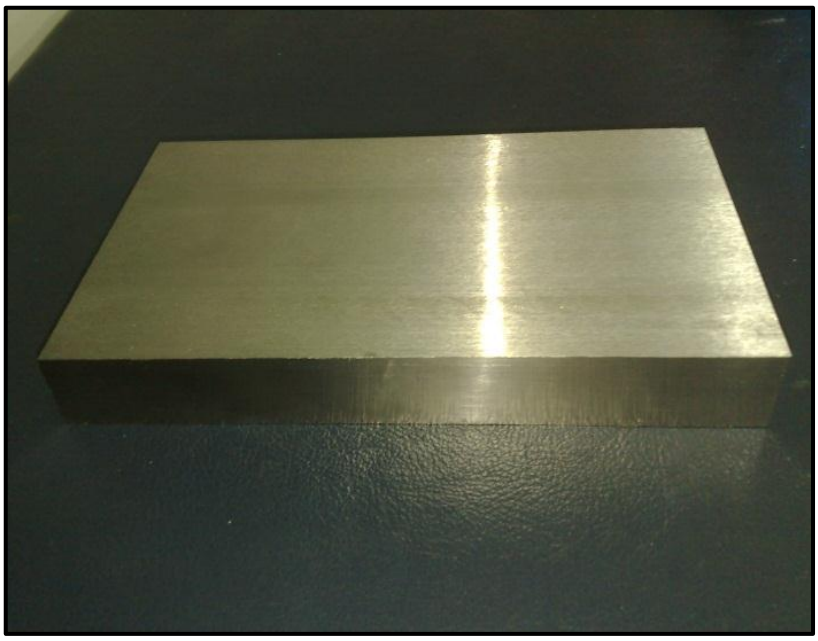

Figure 3.2: The AISI P20 tool steel work piece

Table 3.1: Chemical composition of the AISI P20 tool steel (wt%)

Steel	C	Cr	Ni	Mn	Mo	Si	S	P	Fe
AISI P20	0.37	1.16	1.12	1.42	0.17	0.29	0.008	0.011	Balance

Source: Uslu et al. (2006)

3.3 NANOFLUID PREPARATION

The TiO_2 nanofluid with volume concentration of 0.1% is prepared by single step dilute approach. The method is disperses the measured quantity of nanoparticles into base fluids. The based fluid of the study is distilled water. The 3 bottle of TiO_2 nanofluid procured from SIGMA ALDRICH Company was claimed to be having 35 wt% of nanoparticles per bottle. Figure 3.3 show the nanofluid purchased from SIGMA ALDRICH Company. Table 3.2 shows the properties of nanofluid supplied by SIGMA ALDRICH. The concentration of the nanofluid expressed in terms of volume percent, $\emptyset$ is estimated with Eq. (3.1). The equivalent value of volume percent concentration is shown in Table 3.1.

The expression for conversion wt%, φ to vol%, $\emptyset$ show in Eq. (3.1) is shown below:

$$\emptyset = \frac{\varphi \rho_w}{(1-\varphi)\rho_p + \varphi \rho_w} \quad (3.1)$$

Where, $\emptyset$; the volume concentration of the nanofluid

φ; Weight percentage of the nanoparticles

ρ_w; Density of the distill water

ρ_p; Density of the nanoparticles

By substituting the weight percentage of the nanoparticles, φ = 0.35, density of distilled water, ρ_w= 1000 kg/m^3 and density of the nanoparticles, ρ_p = 4175 kg/m^3, the volume concentration of the nanofluid, $\emptyset$ is calculated as 0.1142 or 11.42 %.

Figure 3.3: TiO_2 nanofluid purchased from SIGMA ALDRICH Company

Table 3.2: Properties of nanofluid supplied by Sigma Aldrich

Type of Nanofluid	Diameter (nm)	Weight Concentration ω (%)	Volume Concentration ϕ (%) using Eq. 3.1
TiO_2	150	35	11.42

Table 3.3: Physical properties of nano materials

Nanoparticle	Thermal Conductivity, W/mK	Density,kg/m^3	Specific heat, J/kgK
TiO_2	8.4	4175	692

Source: Pak and Cho (1998)

The properties of the nanoparticle are listed in Table 3.2. The required volume concentration can be estimated by adding distilled water to the existing nanofluid available in volume percent concentration using the relations given by Eq. (3.2).

The expression for total amount distill water to be added to obtain the required volume concentration of nanofluid show in Eq. (3.2) is shown below:

$$\Delta V = V_1(\frac{\emptyset_1}{\emptyset_2} - 1) \quad (3.2)$$

Where, $\Delta V = V_2 - V_1$; volume of distilled water added into the nanofluid

V_1; initial volume

V_2; final volume

$\emptyset_1$; Volume percentage before dilution

$\emptyset_2$; Volume percentage after dilution

Since the volume concentration of 0.1 % is adequate and the study does not consider the effect of nanofluid concentration, hence the concentration of the TiO_2 nanofluid is decided to be 0.1 %. By substituting V_1 = 225 ml, $\emptyset_1$= 0.1142, $\emptyset_2$ = 0.001, the total volume of distilled water added into the nanofluid is calculated as ΔV = 25 470 ml. Aquamatic Water Still machine is used to prepare the distilled water for the single step dilution approach. Figure 3.4 shows the Aquamatic Water Still machine during the preparation of distilled water.

Figure 3.4: Aquamatic Water Still machine

After the preparation of the distilled water, the TiO_2 nanofluid procured from SIGMA ALDRICH disperses into the prepared distill water. The mixture is then undergoing the stirring process by the motorized stirrer for 1hour with 1000rpm speed. After the stirring process, the nanofluid is then keep in a container for two weeks in order to observed the stability of the nanofluid. If the produced nanofluid is not stable, the nanoparticles will agglomerate at the bottom of the container. The nanofluid preparation procedure need to repeat again with different volume concentration of nanofluid until form a stable state diluted TiO_2 nanofluid. The Figure 3.5 shows the stirring process and the prepared TiO_2 nanofluid. After two weeks of observation, the prepared TiO_2 nanofluid is ready to be used for conducting the grinding experiments as there are no sign of nanoparticles agglomerate at the bottom of the container.

(a) (b)

Figure 3.5: (a) Stirring process; (b) The prepared TiO_2 nanofluid

3.4 GRINDING EXPERIMENTS

3.4.1 Grinding Machine

The grinding machine of Precision Surface Grinder is used to conduct the experiments. The model of the Precision Surface Grinder is STP-1022 ADC II from Supertec, Japan show in Figure 3.6. Table 3.4 shows the machine specification of the grinding machine. The axial cutting depth can be adjusted manually. The work table speed, v_s and grinding wheel speed, v_w are held constant throughout the experiments. The flow rate of coolant is maximized and held constant throughout the experiment is conducted.

Figure 3.6: Supertec Precision Surface Grinder STP-1022 ADC II

Table 3.4: Machine specifications of grinding machine model STP-1022 ADC II

Machine Specifications	
Table Size	200 x 500 mm
Maximum Grinding Length	550 mm
Maximum Grinding Width	210 mm
Maximum Table Load	300 kg
Standard Magnetic Chuck Size	200 x 500 mm
Wheel Size	205 x 22 x 32 mm
Wheel Speed	2850 rpm
Spindle Motor	2 hp
Crossfeed Motor	40W/ 80W
Elevating Motor	¼ hp
Hydraulic Motor	1 hp

3.4.2 Grinding Wheels

The grinding wheels used for conducting the experiments are Al_2O_3 grinding wheel and SiC grinding wheel. Table 3.5 shows the composition for the wheels and Figure 3.7 show the aluminium oxide grinding wheel and silicon carbide grinding wheel.

Table 3.5: Chemical composition of the grinding wheels (wt%)

Type of wheels	Al_2O_3	SiO_2	Fe_2O_3	TiO_2	SiC	F.C.
Aluminium Oxide	95% min	1% max	0.3% max	3% max	-	-
Silicon Carbide	-	-	0.2% max	-	99% min	0.5% max

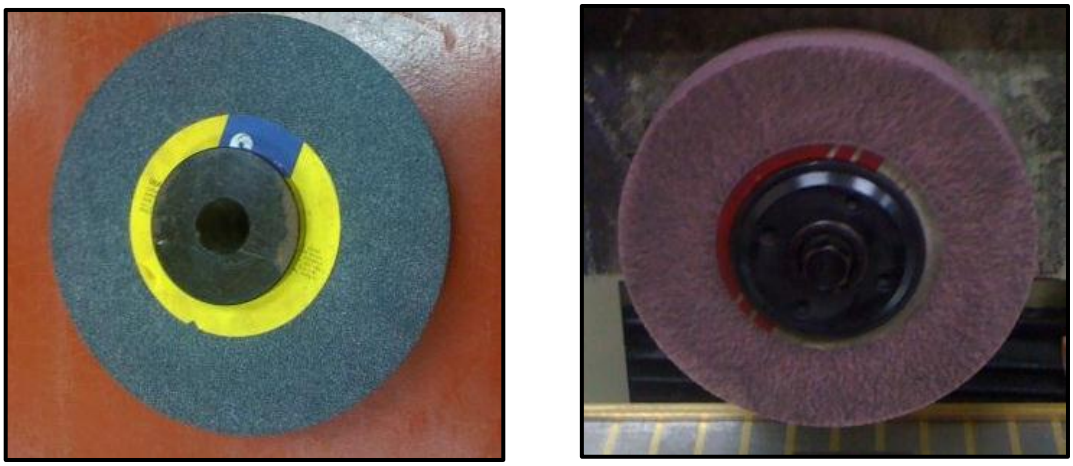

(a) (b)

Figure 3.7: (a) Aluminum Oxide and (b) Silicon Carbide Grinding wheel

3.4.3 Design of Experiments

The grinding processes are conducted by using 2 type of cutting fluid which are water based coolant and TiO_2 nanofluid. For the water based coolant, two different type of wheel were used which are Al_2O_3 wheel and SiC wheel. For each type of wheel, the grinding processes are conducted in conditions of single pass grinding and multi passes grinding. For each type of grinding setup, different depth of cut is manipulated to investigate the relationship between depths of cut with the surface roughness. The manipulated depths of cut for each grinding setup are 5 µm, 7 µm, 9 µm, 11 µm, 13 µm,

15 µm, 17 µm, 19 µm, 21 µm. On the other hand, the grinding processes using TiO_2 nanofluid are only conducted with SiC wheel. There are the same grinding methods of single pass grinding and multi passes grinding for the TiO_2 nanofluid. Each grinding setup with TiO_2 nanofluid undergoes the same manipulated axial cutting depth with the water based coolant grinding depths of cut. The arithmetic surface roughness, *Ra* is then measured on the grounded area. Figure 3.8 illustrate the design of experiment for each type of grinding setup. The total number of conducted grinding experiments is 54 set experiments.

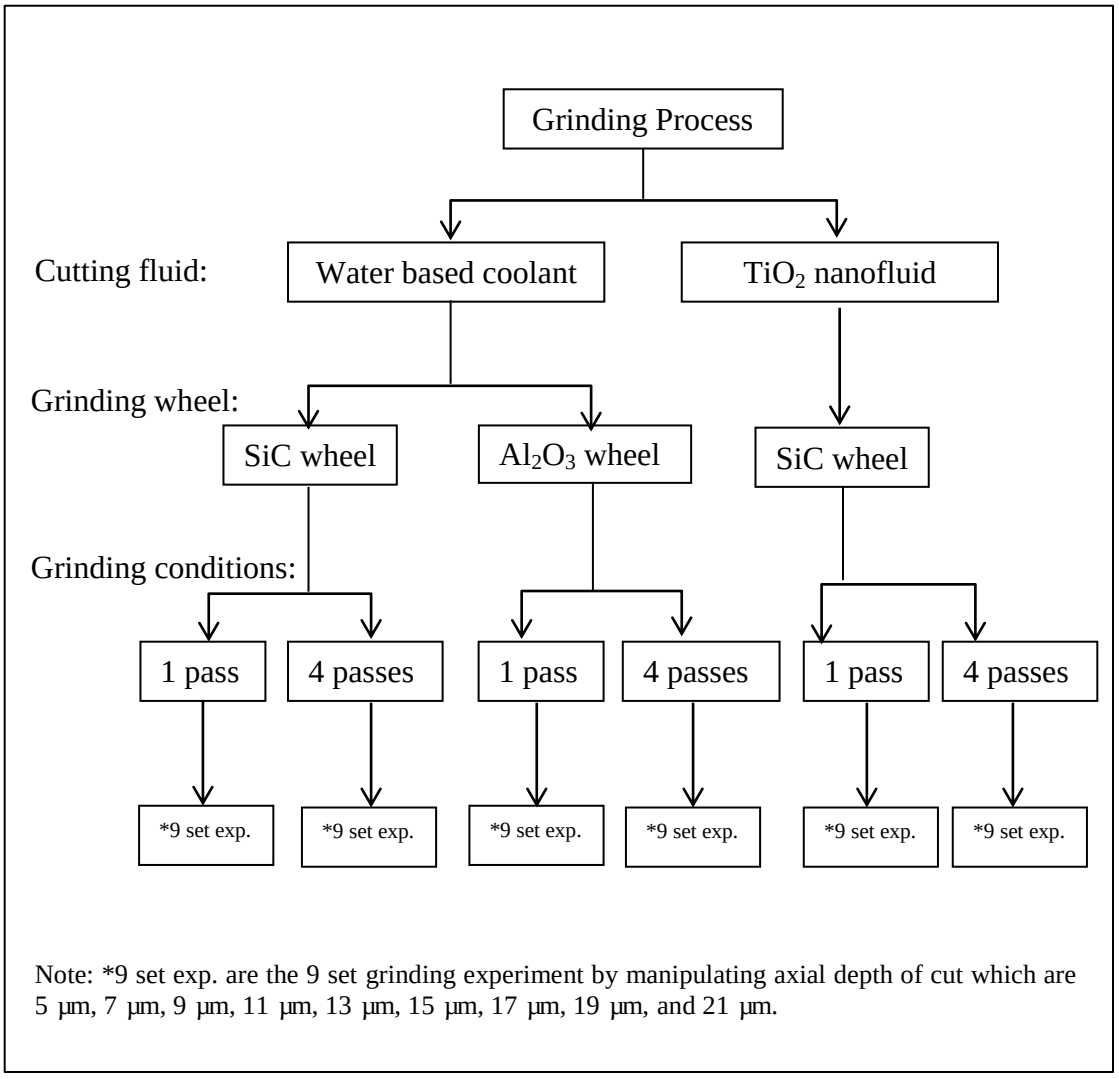

Figure 3.8: The design of experiment for each type of grinding setup

3.4.4 Experiments Procedure

The grinding experiments start with the dressing and truing the wheel for conditioning the surface sufficient for the wheel to cut at the required performance level. The diamond wheel dresser is used to dress the grinding wheel. Dressing is carrying out before every experiment. This is because the debris on the wheel will affect the experimental results. After the wheel dressing, the wheel diameter is measured. Figure 3.9 shows the diamond wheel dresser which is used for wheel dressing.

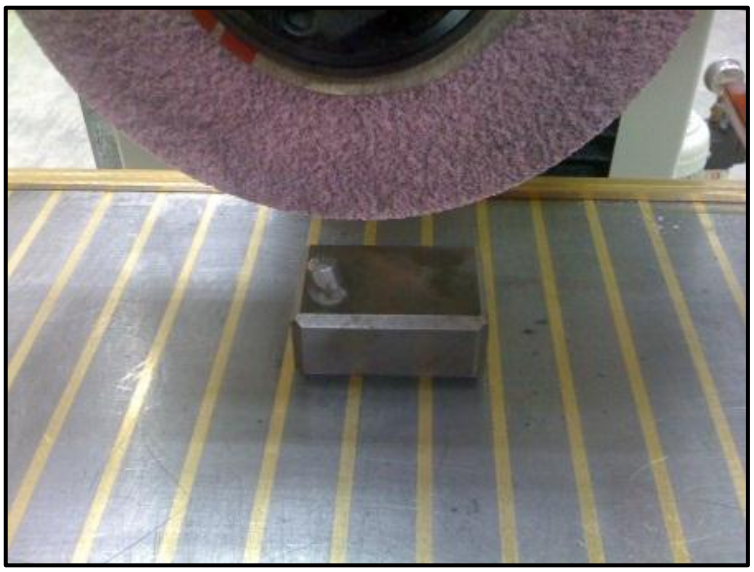

Figure 3.9: Diamond wheel dresser

Since AISI P20 tool steel contain alloying element, hence the machine's magnetics system has no effect on the work piece. Steel clampers are used to hold the work piece and minimize the vibration during the grinding process. Figure 3.10 show the work piece clamp by the steel clampers during the grinding process.

Figure 3.10: The steel clampers used to clamp the work piece during the experiment

The work table speed, v_s and wheel speed, v_w are held constant throughout the experiments. The work table speed, v_s set to be 20 m/min where the wheel speed, v_w is unchangeable for the grinding machine which is 2850 rpm. Tachometer is used to help the adjustment of the work table speed since the grinding machine has no indicator of the work table speed. The tachometer is used to measure the constant work table speed every time just before the grinding experiments conducted. Figure 3.11 shows the tachometer.

Figure 3.11: Tachometer

After the dressing and the work table speed setup, the work piece undergo the grinding process with various axial cutting depths which are 5 µm, 7 µm, 9 µm, 11 µm, 13 µm, 15 µm, 17 µm, 19 µm, 21 µm. For example, the single pass grinding using SiC wheel is conducted after the setting of depth of cut to 5 µm. The wheel diameter and the arithmetic average roughness parameter, *Ra* of the grounded area are measured. The wheel diameter is measured by using the measuring instrument of Vernier caliper which provide a precision to 0.01 mm and reading error of 0.05 mm. The measured data are recorded. Repeat the experiment with the different depth of cut by the same experiment procedure. For the multi passes grinding, the passes are set to be 4 passes. The grinding procedure for the different grinding wheel, different cutting fluids are the same.

3.4.5 Surface Roughness Measurement

Mahr Perthometer S2 is used to measure the surface roughness of the grounded area. Total three measurements were taken for each grounded area in three different positions. The measured arithmetic average roughness parameter, *Ra* used to analyse the surface roughness of the grounded area. Figure 3.12 show the Mahr Pethometer S2.

Figure 3.12: Mahr Perthometer S2

3.5 METALLOGRAPHIC ANALYSIS

Surface integrity of the machined surfaces and subsurface damage were assessed using a scanning electron microscope (SEM). The microstructure analysis was conducted on the selected samples. Six samples were choosing from the grinding experiment using SiC wheel with water based coolant and TiO_2 nanofluid. Three different cutting depths of 5 µm, 11 µm and 21 µm from each experiment have been chosen for metallographic analysis. The total six samples were observed in the as-machined condition. Cutting process is necessary since the work piece is too large and it is not suitable for the SEM analysis. Selected samples were sectioned for the ease of observation on SEM. **T**he samples were cut into small pieces with the dimension of 30 mm x 30 mm x 20 mm. SEM is used to generate high-resolution images of shapes on the work piece after perform the grinding process. The SEM model is Carl Zeiss AG EVO 50 Series. Figure 3.13 shows the SEM model Carl Zeiss AG EVO 50 Series which is used for the metallographic analysis of the project.

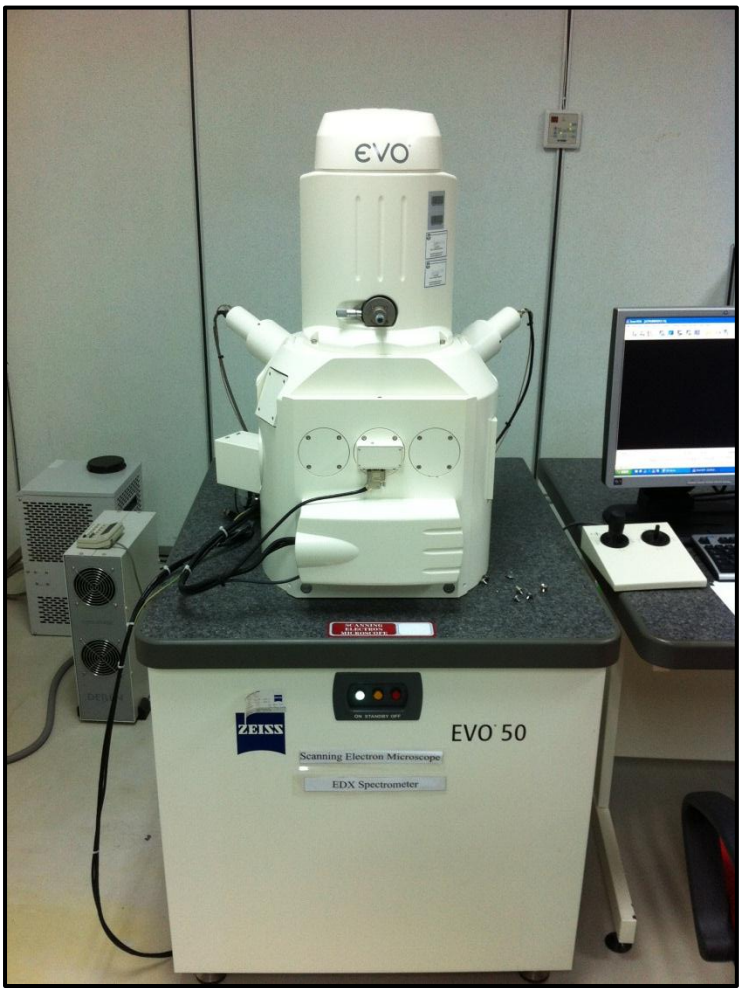

Figure 3.13: SEM model Carl Zeiss AG EVO 50 Series

3.6 ARTIFICIAL NEURAL NETWORK DATA MODELLING

Artificial Neural Network (ANN) is a mathematical model or computational model. ANN is usually used to model complex relationships between inputs and outputs or to find patterns in data. In this project, ANN is used to model and forecast the result of surface roughness from the generated result of grinding experiments. The software which used to model the data is Alyuda NeuroIntelligence. The collected data of each experiment become the input dataset for the ANN. After import the data into the software, the data will be assigned as training (TRN), testing (TST) and validation (VLD) mode. The depth of cut is selected as the input where surface roughness is selected as output in order to model the results. Table 3.6 shows the analyzing dataset of Alyuda NeuroIntelligence.

Table 3.6: The analyzing dataset of Alyuda NeuroIntelligence

	(N) Depth of Cut	(N) Surface Roughness
TRN	5	0.355
TRN	7	0.379
TRN	9	0.441
TST	11	0.523
TRN	13	0.672
TRN	15	0.701
TRN	17	0.899
TRN	19	0.941
VLD	21	1.092

Two neurons and one hidden layer will be selected to design the network for setting of the architecture design of the neurons. Figure 3.14 shows the image of the network with two neurons and one hidden layer.

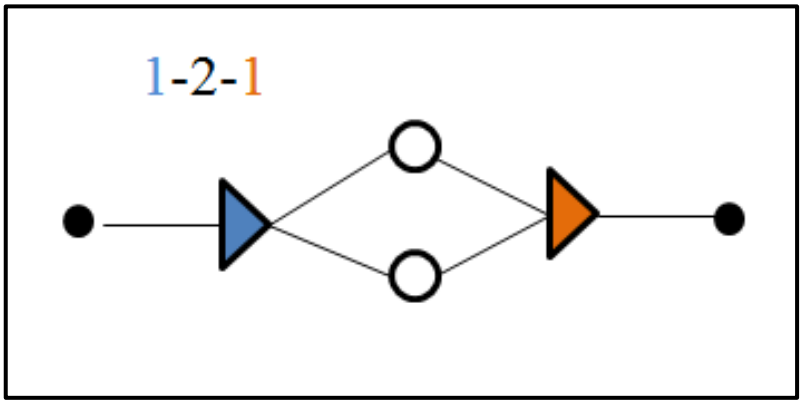

Figure 3.14: Image of the Network

Furthermore, Heuristic Search method is selected as the architecture search option. Then, the fitness criteria are changed to R-squared and the iteration is set to 1000. Furthermore, the automatically select the best network icon is clicked. Next, the data will undergo training. For the network training option, Batch back propagation training algorithm is chosen. Then, the stop training condition is set by error value with the Mean Square Error (MSE) of 1×10^{-6}. Table 3.7 shows the network training option.

Table 3.7: Network Training Option

Network Training Option	Criteria
Training Algorithm	Batch Back Propagation
Stop Training Condition	MSE of 1×10^{-6}

After the network training section, the tested result is modeled. The correlation and the R-squared value for the ANN model must be higher than 0.85. The network is trained until the correlation and the R-squared value higher than 0.85. The manual query used to obtain the predicted result of the surface roughness for cutting depth between 21 µm to 50 µm. Finally, the actual and modelling surface roughness versus cutting depth is plotted.

CHAPTER 4

RESULT AND DISCUSSIONS

4.1 INTRODUCTION

In this chapter, the results of the experiments will be discussed in detailed with the help of the data that is collected throughout the experiments. This experimental based project will be focusing on the surface quality and tool wear data collected from the grinding experiments. The result analyses have been sectionalized into surface roughness analysis, tool wear analysis and SEM micrographs analysis. The effect of the variation axial depth on the grinding surface quality is discussed based on the result of the conducted experiments. The experimental result from the grinding experiments conducted by the using SiC wheel with cutting fluid of water based coolant and TiO_2 nanofluid is then analyzed in order to determine the effect of TiO_2 nanofluid on the grinding surface finish and tool life. The SEM micrograph of each selected specimen is observer and analyzed. The final part of the chapter is discussed on the Artificial Neural Network prediction model.

4.2 SURFACE ROUGHNESS ANALYSIS

4.2.1 Grinding Experiments using Water Based Coolant

The grinding experiments are conducted by using water based coolant as cutting fluid with SiC grinding wheel and Al_2O_3 grinding wheel. The measure arithmetic average surface roughness for each run of experiment is collected. The collected data is plotted into graph. Figure 4.1and 4.2 below shows the graph of surface roughness versus depth of cut for grinding with cutting fluid of water based coolant using SiC

wheel and Al_2O_3 wheel respectively. From the figures, the relationship between surface roughness and the grinding axial depth of cut is observed.

From Figure 4.1, the graph show that the surface roughness increase as the result of increasing of grinding axial depth of cut for the grinding experiment using SiC wheel. The single pass grinding experiments of using SiC wheel has the lowest surface roughness of 0.710 µm when the axial depth of cut is set as 5 µm. The highest surface roughness for the single pass grinding experiments of using SiC wheel is 1.748 µm at the axial depth of cut of 21 µm. The surface roughness has increase 146 % from 0.710 µm to 1.748 µm with the increments of depth of cut from 5 µm to 21 µm.

The multi passes grinding experiments of using SiC wheel has the lowest surface roughness of 0.570 µm at the axial depth of cut of 5 µm. The highest surface roughness for the single pass grinding experiments of using SiC wheel is at the axial depth of cut of 21 µm with the arithmetic average surface roughness value of 1.412 µm. The surface roughness value has increase 148 % from 0.570 µm to 1.412 µm with the increments of depth of cut from 5 µm to 21 µm. Both of the arithmetic average surface roughness for experiment with grinding condition of single and multi passes grinding using SiC wheel show the directly proportional relationship with the grinding axial depth of cut.

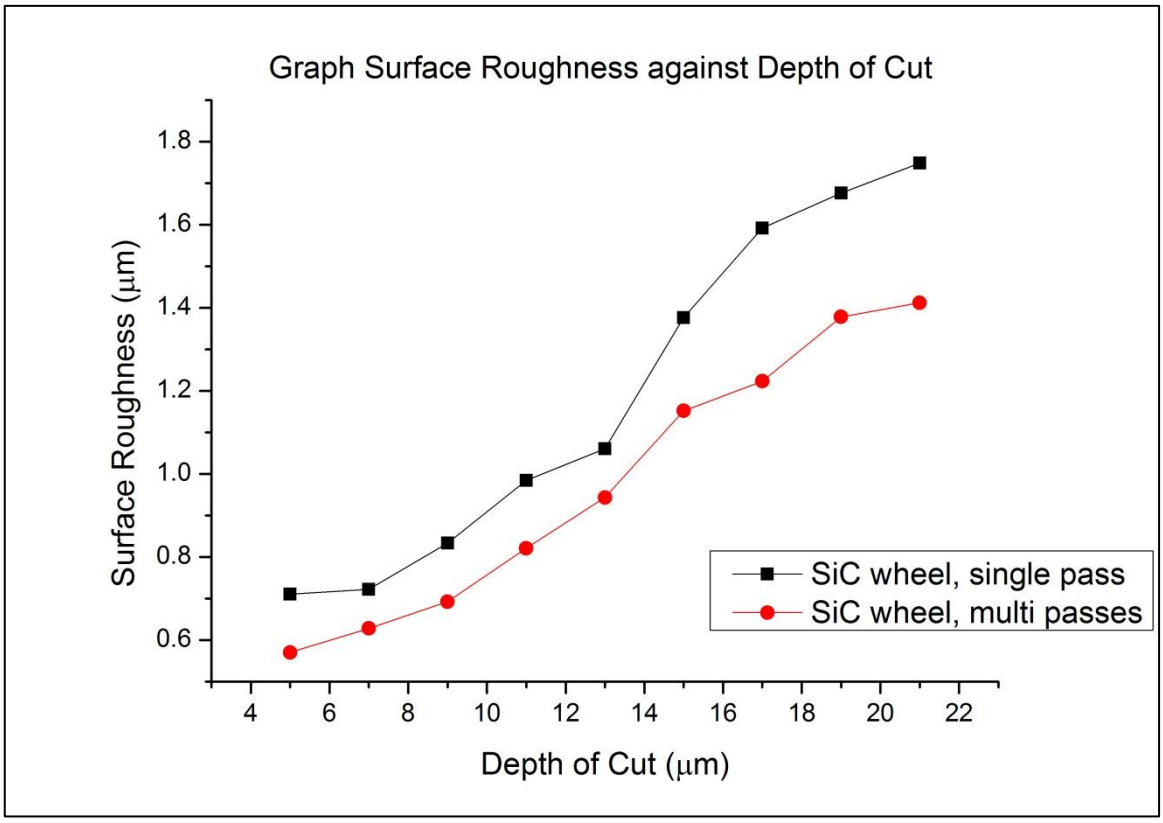

Figure 4.1: Graph of surface roughness versus depth of cut for grinding using SiC wheel with cutting fluid of water based coolant

From Figure 4.2, both of the arithmetic average surface roughness for experiment with grinding condition of single and multi passes grinding using Al_2O_3 wheel also show the directly proportional relationship with the grinding axial depth of cut. The single pass grinding experiments of using Al_2O_3 wheel has the lowest surface roughness of 0.622 μm when the axial depth of cut is set as 5 μm. The highest surface roughness for the single pass grinding experiments of using Al_2O_3 wheel is 1.687 μm at the axial depth of cut of 21 μm. The surface roughness has increase 171 % from 0.622 μm to 1.687 μm with the increments of depth of cut from 5 μm to 21 μm. The results show the increments of the axial depth of cut have increased the surface roughness of the grounded area.

The multi passes grinding experiments of using Al_2O_3 wheel has the lowest surface roughness of 0.529 μm at the axial depth of cut of 5 μm. The highest surface roughness for the single pass grinding experiments of using Al_2O_3 wheel is at the axial

depth of cut of 21 µm with the arithmetic average surface roughness value of 1.293 µm. The surface roughness value has increase 144 % from 0.529 µm to 1.293 µm with the increments of depth of cut from 5 µm to 21 µm.

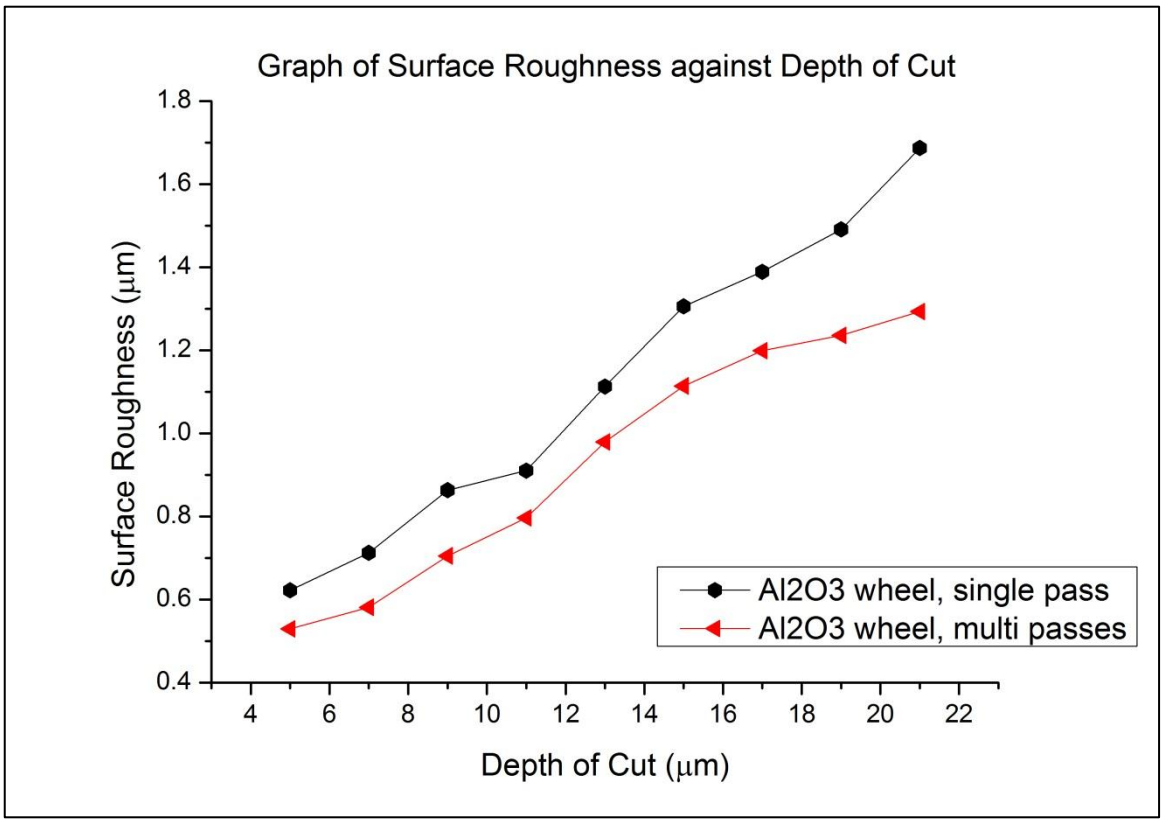

Figure 4.2: Graph of surface roughness versus depth of cut for grinding using Al_2O_3 wheel with cutting fluid of water based coolant

From both Figure 4.1 and 4.2, the graph both showed both of the arithmetic average surface roughness for experiment with grinding condition of single and multi passes grinding using SiC wheel and Al_2O_3 wheel are directly proportional to the grinding axial depth of cut. This indicates that the increment of the depth of cut has resulted the increasing of surface roughness.

The higher the surface roughness imply the worse the surface quality of the grounded area. Hence the surface quality of the work piece is worse with the larger axial grinding depth of cut. The depth of cut is the prominent factor influencing the normal and tangential force components in both the grinding systems. (Prabhu and Vinayagam,

2011) The larger depth of cut requires the higher grinding force. Thus, the friction force between the work piece and the grinding wheel also increase and consequently causing the higher heat generation between the work piece and grinding tool zone. (Krisha et al, 2008) Intense heat generated in grinding due to relatively high frictional effects impairs work piece quality by inducing thermal damage.

Besides that, for lower cutting depth, more grains will participate in material removing hence the depth of engagement is lower and producing smooth surfaces. However, for higher cutting depth the grain that interacts with the work piece will produce the undeformed chip on the work piece surface which caused the rough surface. (Hecker and Liang, 2003) Hence the arithmetic average surface roughness value, *Ra* of the conducted grinding experiments increased with the increments of the axial depth of cut.

4.2.2 Grinding Experiments using TiO_2 Nanofluid

The grinding experiments conducted by using SiC grinding wheel with TiO_2 nanofluid as cutting fluid are comparing with the grinding experiments conducted with water based coolant. The collected data of measured arithmetic average surface roughness, *Ra* for each run of experiment is plotted into graph. Figure 4.3 below shows the graph of surface roughness versus depth of cut for grinding using SiC wheel with cutting fluid of water based coolant and TiO_2 nanofluid. From the figure, the effect of TiO_2 nanofluid on the grinding surface quality compared with the water based coolant is discussed.

From Figure 4.3, both of the arithmetic average surface roughness for experiments grinding with cutting fluid of TiO_2 nanofluid shows the lower value than the experiments grinding with cutting fluid of water based coolant. The multi passes grinding experiment with TiO_2 nanofluid show the lowest value of arithmetic average surface roughness when compared to the multi passes grinding experiment with water based coolant. The multi passes grinding experiments with TiO_2 nanofluid has the lowest surface roughness of 0.355 µm with a 38 % decrement compare to the grinding experiments with water based coolant of 0.570 µm at axial depth of cut 5 µm. The

highest surface roughness for the multi passes grinding experiments of using TiO_2 nanofluid as cutting fluid is 1.092 μm at the axial depth of cut of 21 μm and has a 23 % decrement when comparing to the surface roughness of grinding experiments with water based coolant, 1.412 μm.

The single pass grinding experiments with TiO_2 nanofluid show the lowest value of arithmetic average surface roughness when compared to the single pass grinding experiments with water based coolant. The single passes grinding experiments with TiO_2 nanofluid has the lowest surface roughness of 0.529 μm with a 34 % decrement compare to the grinding experiments with water based coolant of 0.710 μm at axial depth of cut 5 μm. The highest surface roughness for the multi passes grinding experiments of using TiO_2 nanofluid as cutting fluid is 1.311 μm at the axial depth of cut of 21 μm and has a 33 % decrement when comparing to the surface roughness of grinding experiments with water based coolant, 1.748 μm.

From Figure 4.3, the graph shows both of the arithmetic average surface roughness for SiC wheel grinding experiment with grinding condition of single and multi passes grinding for TiO_2 nanofluid are exhibit the better surface quality than the water based coolant as the arithmetic average surface roughness obtained are lower than the latter. The reduction in surface roughness was observed to be 20% to 40% in grinding condition of TiO_2 nanofluid as cutting fluid.

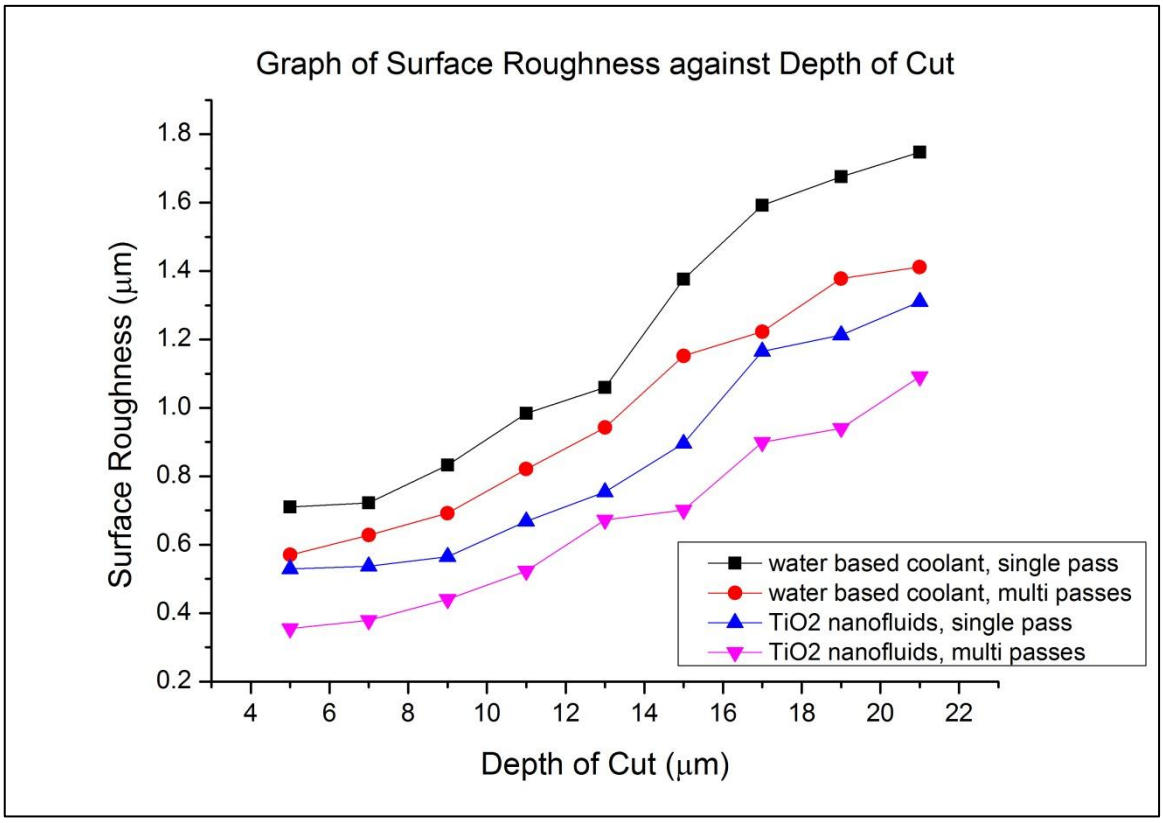

Figure 4.3: Graph of surface roughness versus depth of cut for grinding using SiC wheel with cutting fluid of water based coolant and TiO_2 nanofluid

Cutting fluids with inclusion of nanoparticles have enhanced heat transfer capacity up to 6%. The advanced heat transfer and tribological properties of nanofluids can provide better cooling & lubricating in grinding process. (Saidura et al., 2010) The TiO_2 nanofluid has the better thermal conductivity and heat transfer coefficient compared to the water based coolant which decreases the intensive temperature generated in grinding zones which results in the development of residual stresses, micro-cracking and tempering of the work piece surface.

The fact that the nanofluids outperform the water based coolant can be due to the reduction in grinding forces and friction. The better lubrication effect of TiO_2 nanofluid lower the tangential grinding forces as less rubbing and plowing on the grinding process. Hence the better thermo physical properties of the TiO_2 nanofluid has resulted the better surface finish in grinding as lubrication reduces the cutting forces and cutting energy,

while convection heat transfer and/or boiling carries away the heat generated in the grinding zone.

4.2.3 Influence of Grinding Passes

From Figure 4.1, 4.2 and 4.3, the comparisons between the grinding condition of single pass grinding and multi passes grinding have shown the latter obtain the lower surface roughness value. From the result, it can be noticed that surface roughness show lower value at the larger number of grinding passes. The result show that the multi passes grinding exhibit the better surface quality with the 15 % to 35 % reduction of surface roughness value compared to single pass grinding. This indicates that the multi passes grinding exhibit the better surface quality.

According to Chen and Rowe (1995), grinding process can be distinguished into three phases, including rubbing, ploughing and cutting. Rubbing and ploughing are inefficient as the energy is wasted in deformation and friction with negligible contribution to material removal. The wasted energy may cause the grain engages with the work piece in up-cut grinding, the grain slides without cutting on the work piece surface due to the elastic deformation of the system occur at the single pass grinding. On the other hand, for the multi pass grinding experiment the work piece material piles up to the front and to the sides of the grain to form a groove and complete chips have been performed. This implies that there is a smoothening action on the kerf walls by the second and following pass that removes the ‘peaks’ left by the preceding pass. Hence the multi passes grinding obtain the better surface finish than the single pass grinding.

4.3 WHEEL WEAR ANALYSIS

The wheel wear analysis is conducted on the grinding experiments by using SiC grinding wheel with TiO_2 nanofluid and water based coolant as the cutting fluid. The wheel diameter is measured before and after each run of the grinding experiment. In this research, the wheel wear is accounted as the wheel diameter differences before and after the grinding experiment. The wheel wear is then summing up and differentiate by the grinding condition of number of passes. Figure 4.4 illustrates the wheel wear data

collected from the single and multi passes grinding experiment using SiC wheel with TiO_2 nanofluid and water based coolant as the cutting fluid. From the stack column bar chart illustrates in the Figure 4.4, the comparison between TiO_2 nanofluid and the water based coolant on the grinding wheel wear is analyzed.

From the stack column bar chart illustrates in the Figure 4.4, there is clearly notice that the grinding experiments with TiO_2 nanofluid have no significant effect on the wheel wear. By the measuring instrument of Vernier caliper, provide a precision to 0.01 mm and reading error of 0.05 mm, the wheel diameters are found to be no significant change after each run of grinding experiment with TiO_2 nanofluid conducted. The summing total wheel wear for the water based coolant grinding experiments with grinding condition of single pass is 0.28 mm where multi passes grinding experiment is 0.41 mm.

From the result, the grinding experiment with TiO_2 nanofluid are exhibits the better tool life than the water based coolant as it shown no significant reduction on wheel diameter after the experiments conducted. The grinding wheel wear occurs due to the friction between the abrasive grains and the work piece. (Silva et al., 2005) The enhancement of TiO_2 nanofluid lubricating capacity is attributed to the formation of the slurry layer on the grinding interface which can protect the grinding wheel from grain/bond fracture. It reduces the wear on the grinding wheel by decreasing grain-work piece friction, allowing the abrasive grains to remain bound to the binder for longer periods and leading to lower wear of the tool. The slurry layer generated less wheel wear, smaller grinding forces and better surface finish.

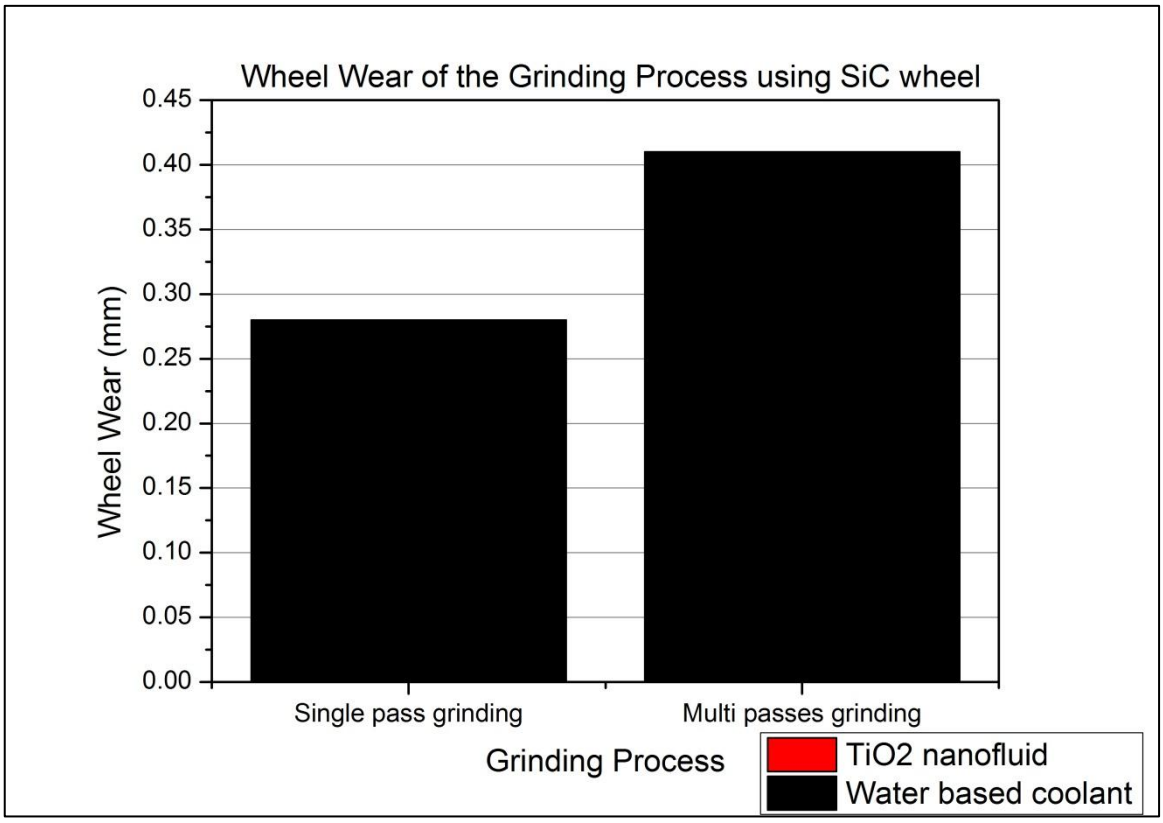

Figure 4.4: Wheel wear of the grinding process using SiC wheel

4.4 METALLOGRAPHIC ANALYSIS

Surface integrity of the machined surfaces and subsurface damage were assessed using a scanning electron microscope (SEM). The microstructure analysis was conducted in the as-machined condition on the selected samples. Six samples were choosing from the grinding experiment using SiC wheel with water based coolant and TiO_2 nanofluid.

4.4.1 Metallographic Analysis on Water Based Coolant Grinding Experiments

Figure 4.5 and Figure 4.6 shows the SEM micrograph of grounded surface of specimen: SiC grinding wheel-water based coolant-4 passes-DOC 5 µm with 250x and 1000x magnification repsectively. From Figure 4.5 and 4.6, the machined surfaces contained characteristic features associated with plastic flow. There are some burning colour found on the work piece surface. The interface temperature is high enough and

the work piece material at the contact zone becomes ductile enough to cause strong welds to form between the abrasive grit and work piece, thereby resulting in the generation of plastically deformed coatings. (Xu et al., 2002) Beside that, it shows continues smooth scratches produced on the grind surface. The scratches are produce by the interactions of abrasive cutting points with the work piece. The scratches are finer as the interactions between the abrasive and the work piece are significantly small for axial depth 5µm. Besides that, the grinding grooves are almost not equally in width and depth.

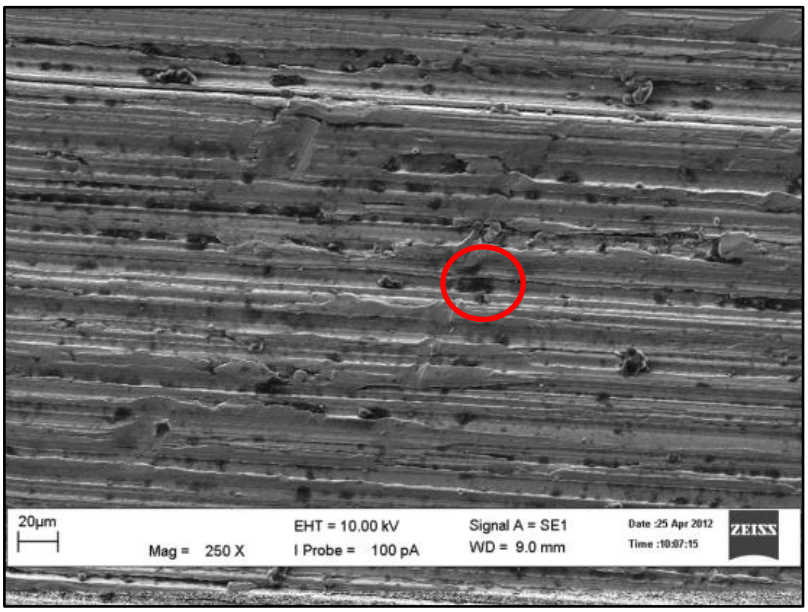

Figure 4.5: SEM micrograph of grounded surface of specimen: SiC grinding wheel-water based coolant-4 passes-DOC 5 µm. 250x magnification

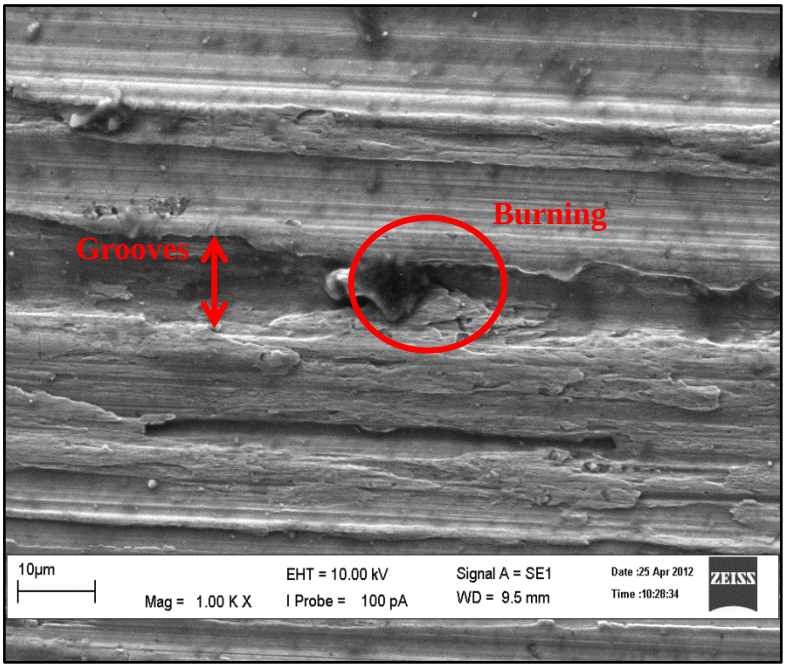

Figure 4.6: SEM micrograph of grounded surface of specimen: SiC grinding wheel-water based coolant-4 passes-DOC 5 µm. 1000x magnification

Figure 4.7 and Figure 4.8 shows the SEM micrograph of grounded surface of specimen: SiC grinding wheel-water based coolant-4 passes-DOC 11 µm with 250x and 1000x magnification repsectively. From Figure 4.7 and 4.8, The machined surfaces contained characteristic features associated with plastic flow, delamination of deformed layer, and side flow across the scratches. There a lot of burning colour occur on the work piece surface compared to Figure 4.5 and Figure 4.6. Since the heat generated in the grinding zone will be higher as the cutting depth is incresesd, therefore, the posibility for burning mark occur on the work piece surface is higher. From the observation of the grooves size, it show that the grooves is unequal in width and depth. Besides that, there are much more overlapping scratches produces compared to the previous.

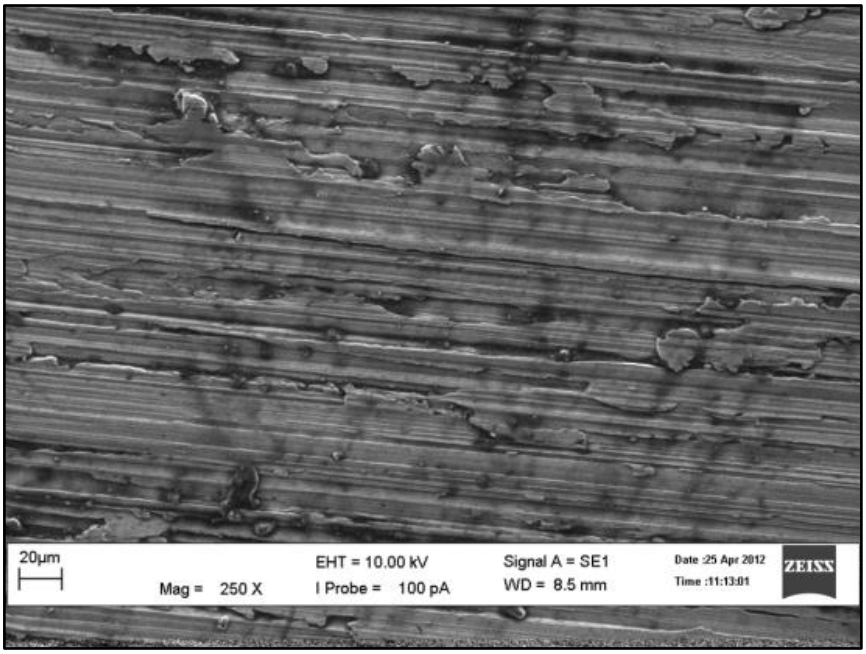

Figure 4.7: SEM micrograph of grounded surface of specimen: SiC grinding wheel-water based coolant-4 passes-DOC 11 µm. 250x magnification

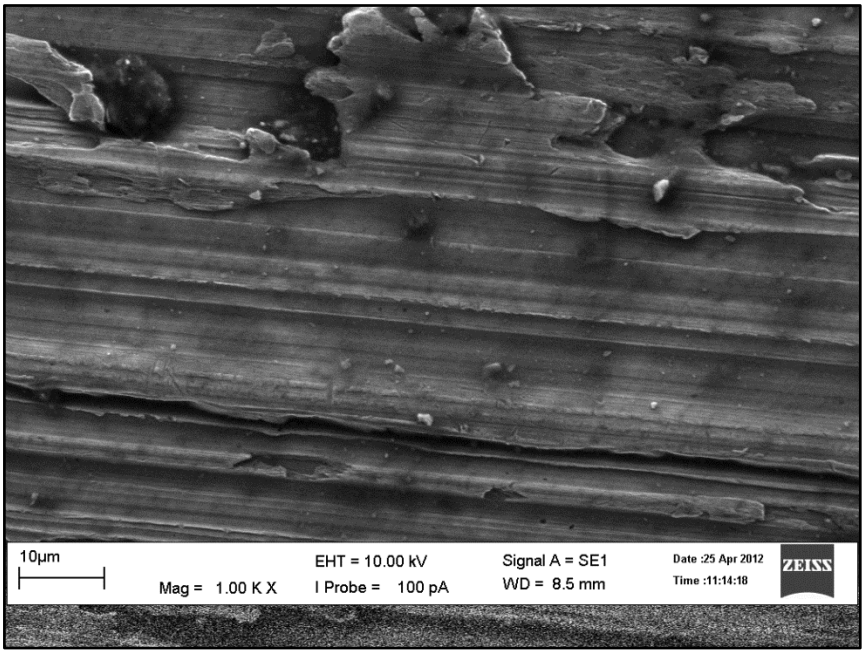

Figure 4.8: SEM micrograph of grounded surface of speciment: SiC grinding wheel-water based coolant-4 passes-DOC 11 µm. 1000x magnification

Figure 4.9 and Figure 4.10 shows the SEM micrograph of grounded surface of specimen: SiC grinding wheel-water based coolant-4 passes-DOC 21 µm with 250x and 1000x magnification repsectively. The surfaces topography shown contained characteristic features associated with plastic flow, delamination of deformed layer, and side flow across the scratches.There are a lot of huge and darker burning colour found on the work piece surface. Further more, the grooves are almost all unequal size and not continues. On the othe hand, there are a lot of raised edges or small pieces of material remaining attached to a work piece which is called burrs on the surface. This contributes to high value of surface roughness. This is happened due to the plastic deformation occur on the surface of the material in conjuction with the thermal effect. (Yan et al., 2009) Besides that, the excessive heat peneterate into the work piece also contribute to the huge amount of burning on the work piece surface.

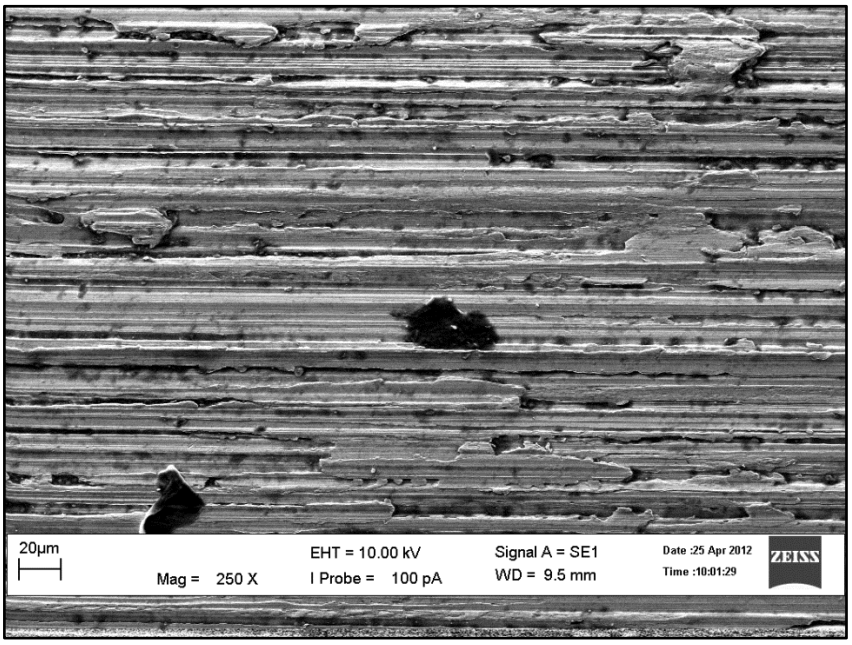

Figure 4.9: SEM micrograph of grounded surface of specimen: SiC grinding wheel-water based coolant-4 passes-DOC 21µm. 250x magnification

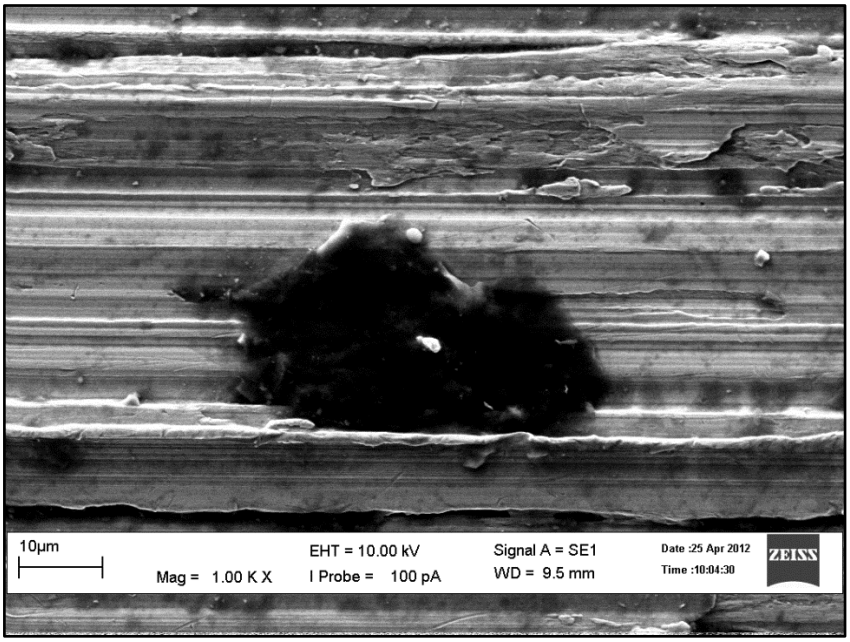

Figure 4.10: SEM micrograph of grounded surface of specimen: SiC grinding wheel-water based coolant-4 passes-DOC 21µm. 1000x magnification

4.4.2 Metallographic Analysis on TiO_2 Nanofluid Grinding Experiments

Figure 4.11 and Figure 4.12 shows the SEM micrograph of grounded surface of specimen: SiC grinding wheel-TiO_2 nanofluid-4 passes-DOC 5 µm with 250x and 1000x magnification repsectively. From Figure 4.11 and 4.12, the SEM micrograph shows almost all normal colour on the image.Besides that, the scractches poduces for cutting depth 5µm are very smooth compared to the Figure 4.3 to Figure 4.8. Further more, the grooves in the finished surface after grind using TiO_2 nanofluid are smoother,wider and also shallower than the material grind using water based coolant. Beside that, there is no burr formation on the surface. These contributes to produce the most finest surface roughness compared to the other experiment. This is due to the high thermal physical properties of TiO_2 nanofluid absorb and remove the heat that penetrate into the work piece during grinding. This phenomena cause the workpiece occur less burning effect. The work piece material removed in the ductile way with no sign of fracture zone shown.

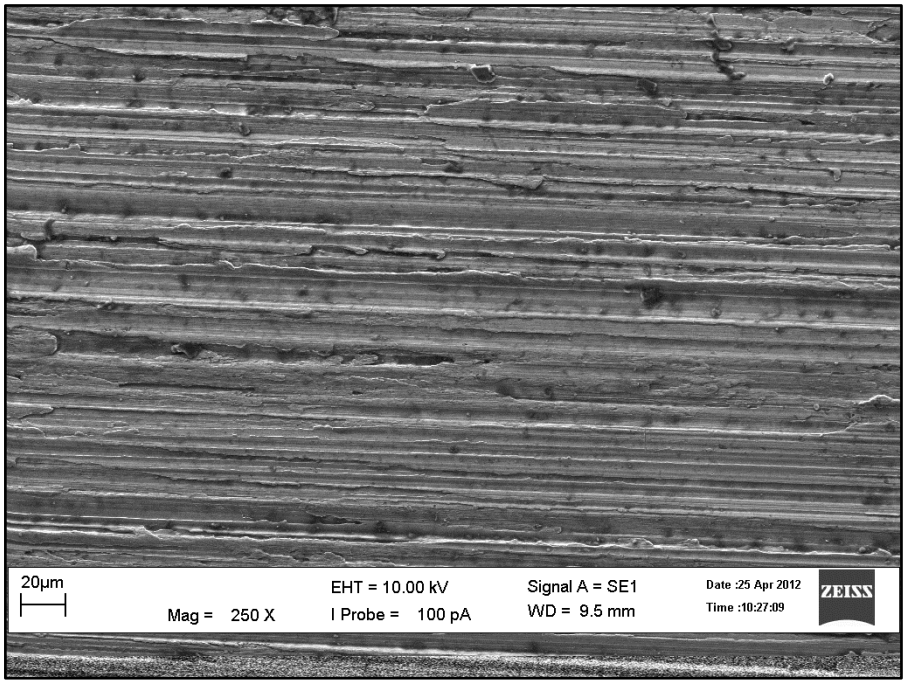

Figure 4.11: SEM micrograph of grounded surface of specimen: SiC grinding wheel-TiO_2 nanofluid -4 passes-DOC 5 µm. 250x magnification

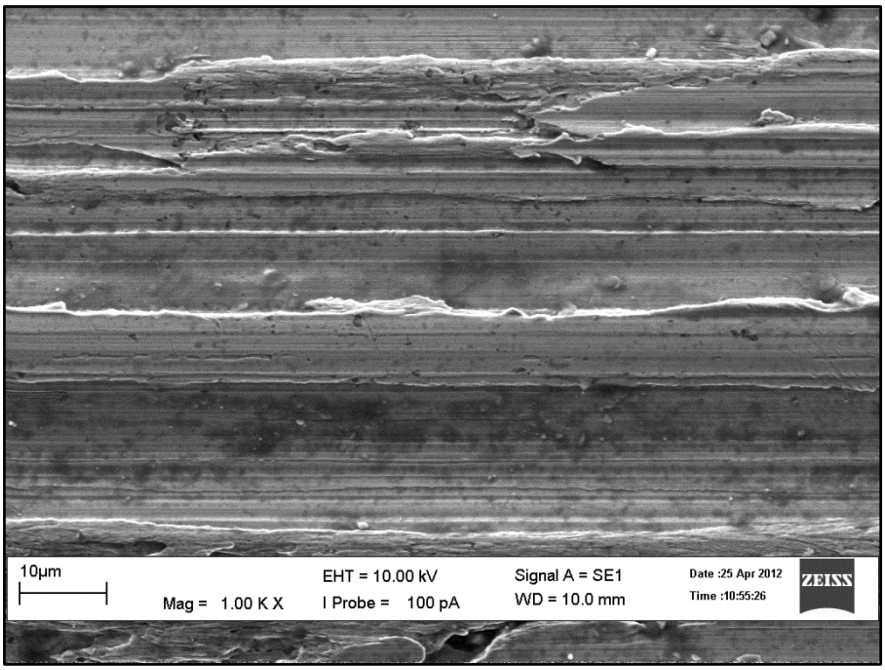

Figure 4.12: SEM micrograph of grounded surface of specimen: SiC grinding wheel-TiO_2 nanofluid -4 passes-DOC 5 µm. 1000x magnification

Figure 4.13 and Figure 4.14 shows the SEM micrograph of grounded surface of specimen: SiC grinding wheel-TiO_2 nanofluid-4 passes-DOC 11 µm with 250x and 1000x magnification repsectively. The results show that the scractches produces by cutting depth of 11 µm are rough compared to the Figure 4.11 and Figure 4.12. Moreover, the grooves are unequal in size and not continueously. On the othe hand, there are a lot of raised edges or small pieces of material remaining attached to a work piece which is called burrs on the surface. Burning mark also found at the machined surface. This contributes to high value of surface roughness. The machined surfaces contained characteristic features associated with plastic flow, delamination of deformed layer, and side flow across the scratches. Besides that, there are many overlapping scratches shown.

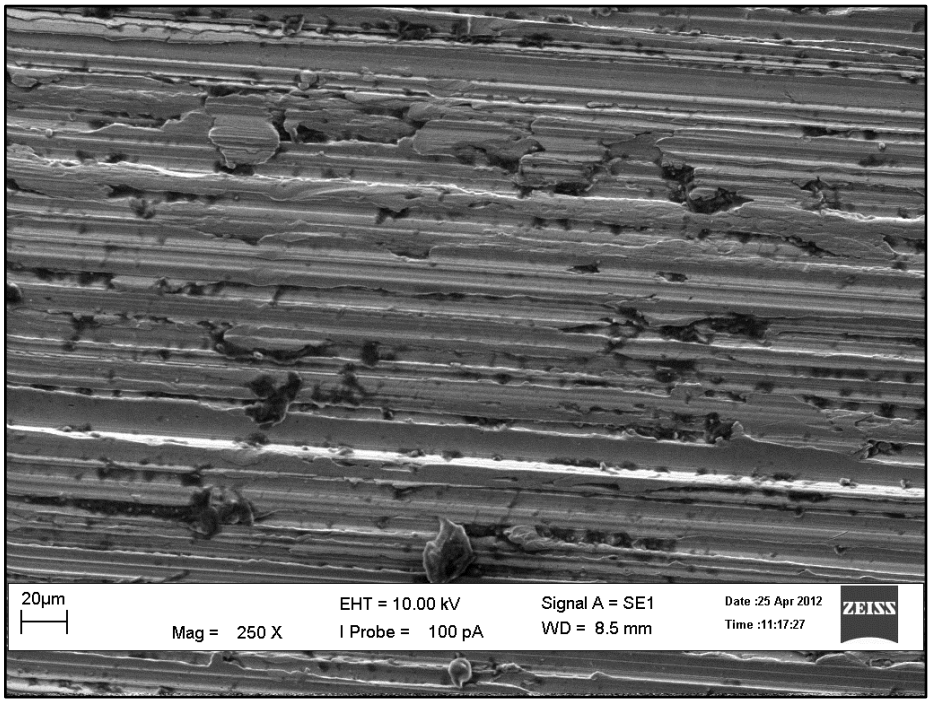

Figure 4.13: SEM micrograph of grounded surface of specimen: SiC grinding wheel-TiO_2 nanofluid -4 passes-DOC 11µm. 250x magnification

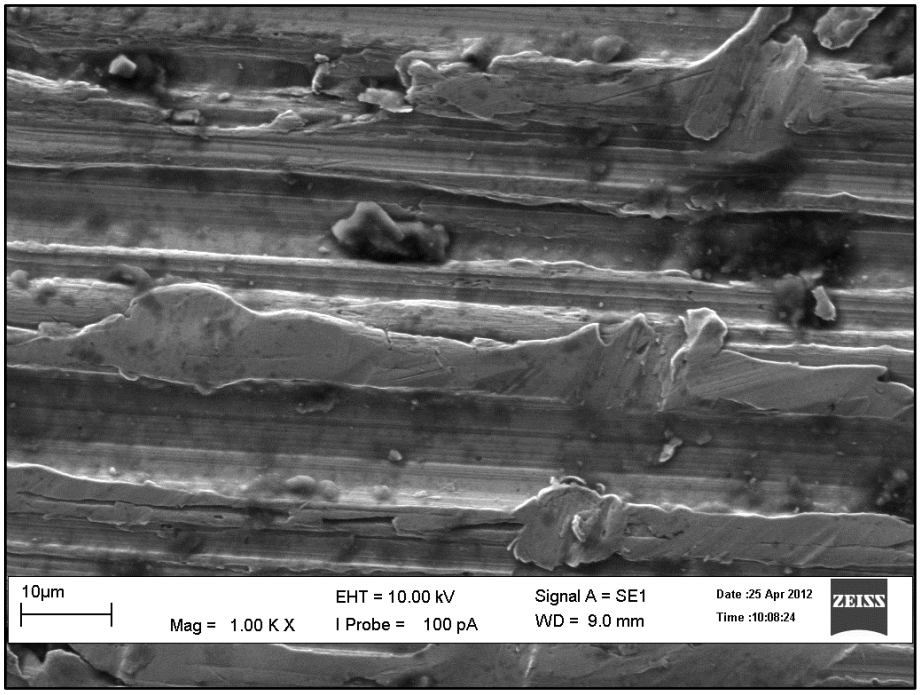

Figure 4.14: SEM micrograph of grounded surface of specimen: SiC grinding wheel-TiO_2 nanofluid -4 passes-DOC 11µm. 1000x magnification

Figure 4.15 and Figure 4.16 shows the SEM micrograph of grounded surface of specimen: SiC grinding wheel-TiO_2 nanofluid-4 passes-DOC 21 µm with 250x and 1000x magnification repsectively. The results shows that the scractches produces for cutting depth 21 µm are very rough compared to the previous figure from Figure 4.11 to Figure 4.14. There appears obvious plastic working trace in the finished surface. The SEM micrograph show the characteristic features associated with plastic flow, delamination of deformed layer, and side flow across the scratches. Moreover, the grooves are unequal in size. Beside that, there are burning color observed from the figure. There are also burr formation along side the grooves.

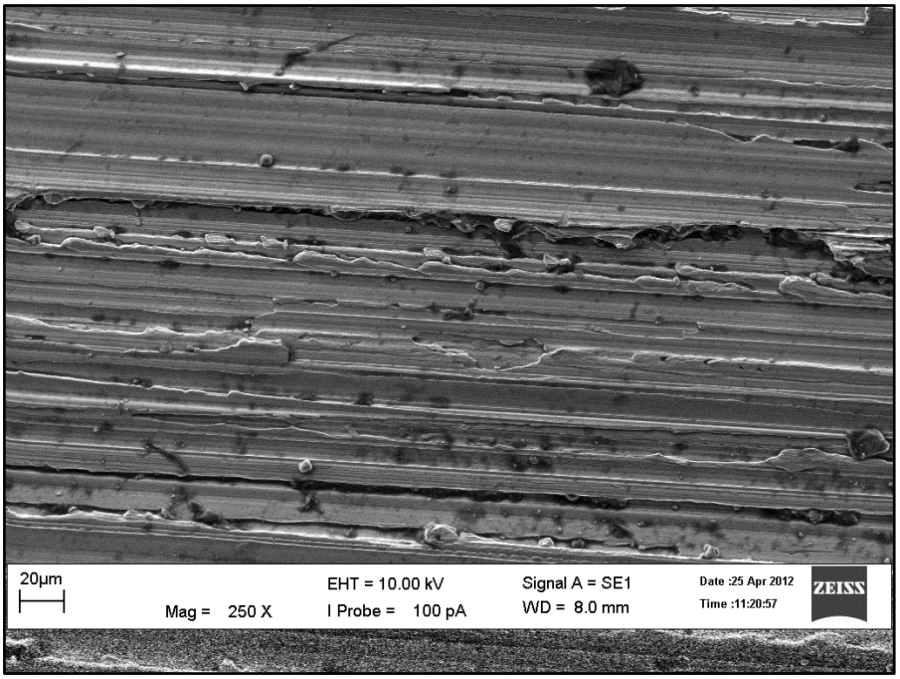

Figure 4.15: SEM micrograph of grounded surface of specimen: SiC grinding wheel-TiO_2 nanofluid -4 passes-DOC 21 µm. 250x magnification

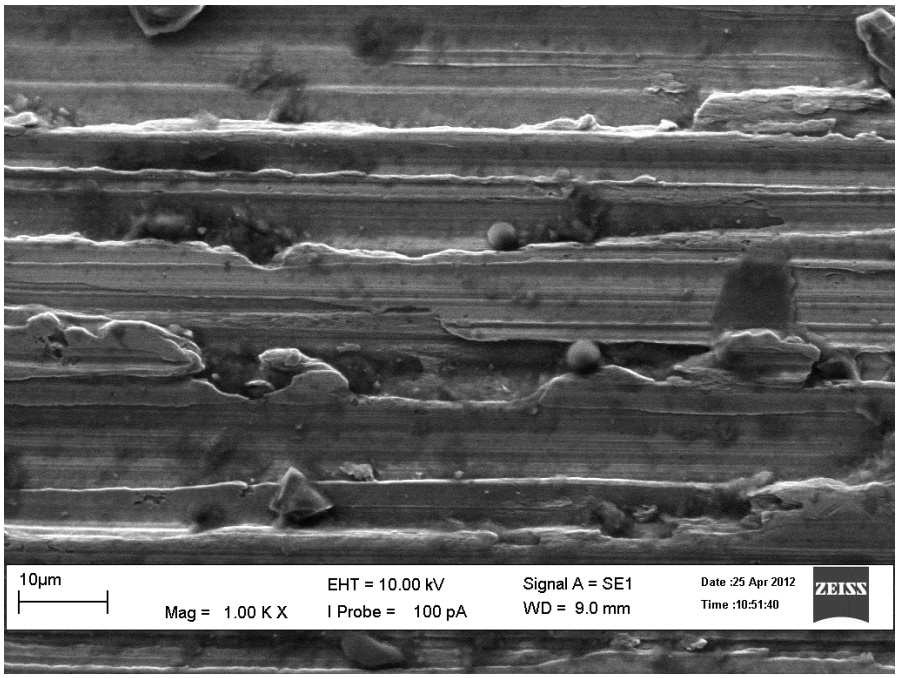

Figure 4.16: SEM micrograph of grounded surface of specimen: SiC grinding wheel-TiO_2 nanofluid -4 passes-DOC 21 µm. 1000x magnification

4.5 ARTIFICIAL NEURAL NETWORK PREDICTION MODELLING

4.5.1 ANN Prediction Modelling on Single Pass Grinding Experiments

The collected data from the grinding experiment with grinding condition of single pass grinding is modeled on the Artificial Neural Network **(**ANN). Figure 4.17 shows the prediction modelling graph using ANN of Surface Roughness versus depth of cut for the conducted single pass grinding experiment.

From the Figure 4.17 shows the ANN prediction modelling graph of Surface Roughness versus depth of cut for single pass grinding experiments. The ANN prediction modelling graph for grinding using water based coolant with SiC wheel has R-squared of 0.9859. Besides that, the ANN prediction modelling graph for grinding using water based coolant with Al_2O_3 wheel has R-squared of 0.968593 and the ANN prediction modelling graph for grinding using TiO_2 nanofluid with SiC wheel has R-squared of 0.988498. R-squared is a statistical ratio that compares model forecasting accuracy with accuracy of the simplest model that just use mean of all target values as the forecast for all records. The closer this ratio to 1 the better the model is. All the R-squared of the prediction model has the value approximately 1 indicates the great forecasting accuracy of the model.

From the prediction model of Figure 4.17, it can be observed that variations on the depth of cut, in its lower range, produce significant changes on the value of the surface roughness. The prediction model results show that there are almost no significant changes on the value of surface roughness after the depth of cut of 21μm. Based on the ANN prediction model, the optimal axial depth of cut can be determined in order to obtain the required surface quality for the work piece.

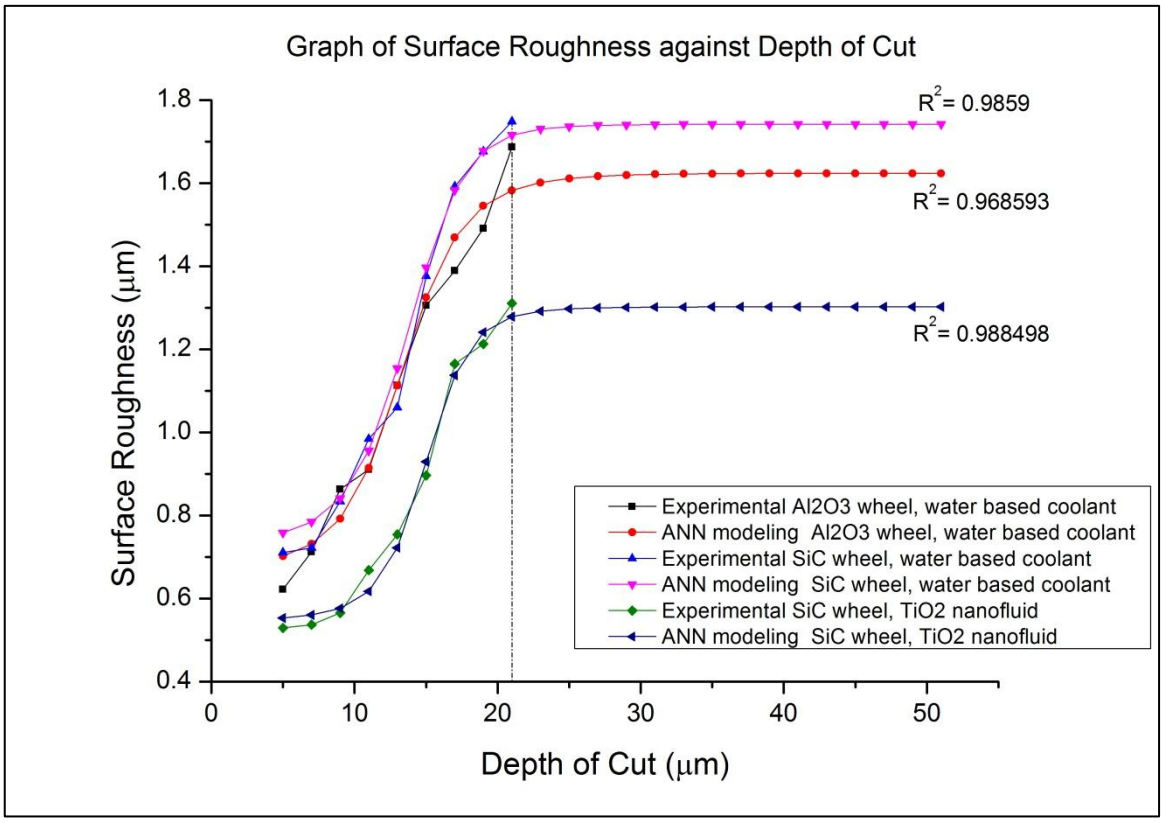

Figure 4.17: Graph of surface roughness against depth of cut for experimental result and Artificial Neural Network Prediction models of single pass grinding

4.5.2 ANN Prediction Modelling on Multi Passes Grinding Experiment

The collected data from the grinding experiment with grinding condition of multi passes grinding is modeled on the Artificial Neural Network **(**ANN). Figure 4.18 shows the prediction modelling graph using ANN of Surface Roughness versus depth of cut for the conducted multi passes grinding experiment.

From the Figure 4.18 shows the ANN prediction modelling graph of Surface Roughness versus depth of cut for multi passes grinding experiments. The ANN prediction modelling graph for grinding using water based coolant with SiC wheel has R-squared of 0.965994. Besides that, the ANN prediction modelling graph for grinding using water based coolant with Al_2O_3 wheel has R-squared of 0.969402 and the ANN prediction modelling graph for grinding using TiO_2 nanofluid with SiC wheel has R-

squared of 0.927595. All the R-squared of the prediction model has the value approximately 1 indicates the great forecasting accuracy of the model.

From the prediction model of Figure 4.18, it also can be noticed that variations on the depth of cut, in its lower range, produce significant changes on the value of the surface roughness. The prediction model results show that there are almost no significant changes on the value of surface roughness after the depth of cut of 21 µm. Based on the ANN prediction model, the optimal axial depth of cut can be determined in order to obtain the required surface quality for the work piece. All of the modelling ANN prediction models by Batch Back Propagation training algorithm have shown with the 90 % above forecasting accuracy.

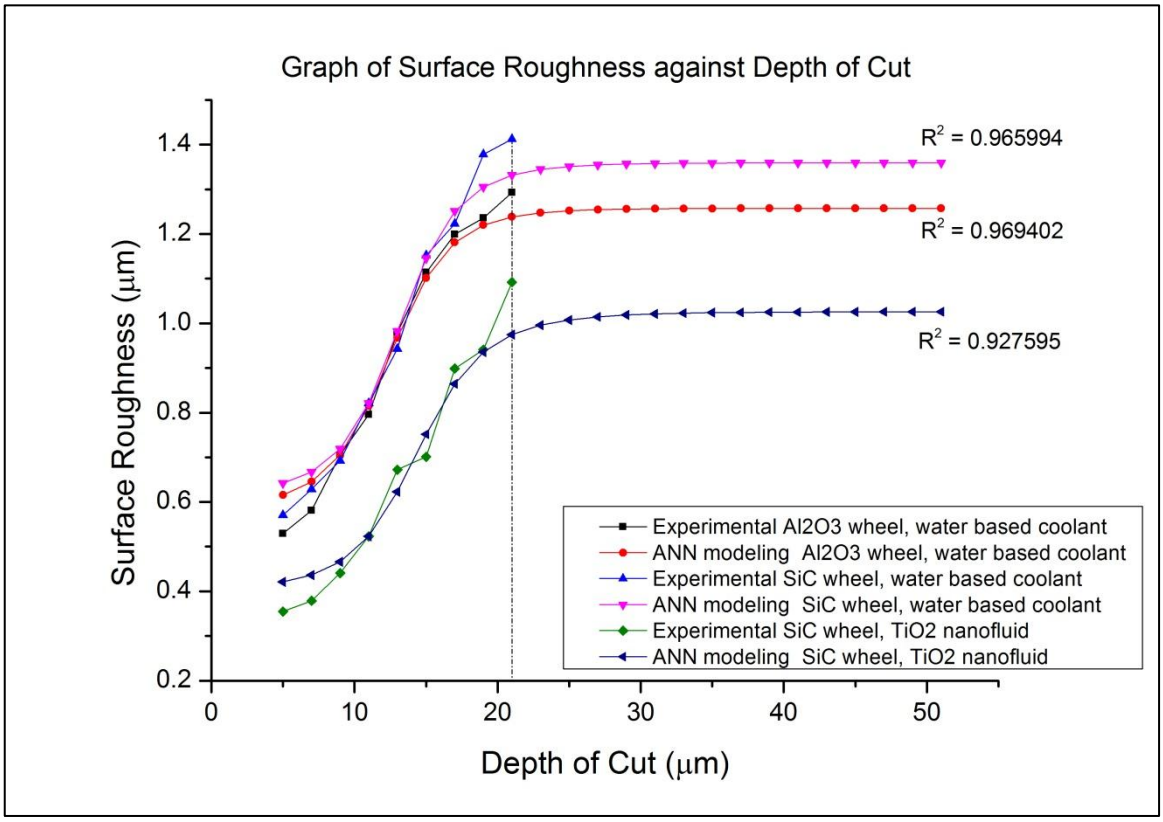

Figure 4.18: Graph of surface roughness against depth of cut for experimental result and Artificial Neural Network Prediction modelling on multi passes grinding

CHAPTER 5

CONCLUSION AND RECOMMENDATIONS

5.1 CONCLUSIONS

The conclusions are made from the analysis undertaken with single pass and multi passes grinding experiments using SiC wheel and Al_2O_3 wheel with water based coolant and TiO_2 nanofluid as cutting fluids.

From the result shown in Chapter 4, it can be concluded that the increments of the axial depth of cut have increased the surface roughness of the grounded area. The surface roughness value is directly proportional to the depth of cut. The result indicates that the better surface quality of the work piece can be obtained at the lower depth of cut.

Moreover, grinding with TiO_2 nanofluid exhibit the better grinding surface quality than the water based coolant. The reduction in surface roughness was observed to be 20% to 40% in grinding condition of TiO_2 nanofluid as cutting fluid when compared to the water based coolant. Grinding with TiO_2 nanofluid has led to the better 20 % to 40 % surface quality than the water based coolant.

The grinding experiment with TiO_2 nanofluid are exhibits the better tool life than the water based coolant as it shown no significant reduction on wheel diameter after the experiments conducted. The summing total wheel wear for the water based coolant grinding experiments with grinding condition of single pass is 0.28 mm where multi passes grinding experiment is 0.41 mm.

Besides that, the comparisons between the grinding condition of single pass grinding and multi passes grinding have shown the latter obtain the lower surface

roughness value. The result show that the multi passes grinding exhibit the better surface quality with the 15 % to 35 % reduction of surface roughness value compared to single pass grinding.

Finally, the 90 % above forecasting accuracy of prediction model are modelling by ANN. The prediction models show that there are almost no significant changes on the value of surface roughness after the depth of cut of 21 µm. Based on the ANN prediction model, the optimal axial depth of cut can be determined in order to obtain the required surface quality for the work piece.

5.2 RECOMMENDATIONS FOR FUTURE RESEARCH

Following recommendation can be implemented for future research and development on grinding machinability using nanofluids.

i. Experiments are to be conducted by determine the effect of variation axial depth on the grinding temperature to experimentally validate the analyzed phenomenon.

ii. Experiments to investigate the different concentrations of nanofluids on the grinding machinability.

iii. Experiments to be conducted by varying the work table speed and axial depth of cut.

iv. The effect of nanofluid as cutting fluids on the other type of machining is to be investigated.

REFERENCE

Agarwal, S. and Rao, P.V., 2007. Improvement in productivity in SiC grinding. *Journal of Engineering Manufacture*, pp. 38-45.

Aguiar, P.R., Cruz, C.E.D., Paula, W.C.F. and Bianchi, E.C. 2008. Prediction surface roughness in grinding using neural networks. *Advance in Robotics, Automation and Control*, **16**(9), pp. 432

Aguair, P.R., Dotto, F.R.L. and Bianchi, E.C. 2005. Study of thresholds to burning in surface grinding process. *Journal of Braz Society of Mechanical Science and Engineering*, **27**(2), pp. 150-156.

Bhatesa, C.P., Chisholm, A.W.J., and Pattinson, E.J. 1972. Advance grinding technology. *Proceeding of the International Grinding Conference*, pp. 334-339.

Brinksmeier, E., Heinzel, C. and Wittmann, M. 1999. Friction and lubrication in grinding. *Journal of Manufacturing Technology*, **48**(2), pp. 581-598.

Buttery, T.C., Statham, A., Percival, J.B. and Hamed, M.S. 1979. Some effect of dressing on grinding performance. *Journal of Mechanical and Production Engineering*, **55**(1979), pp. 195-219.

Chen, X., Allanson, D.R. and Rowe, W.B. 1998. Life cycle model of the grinding process. *Journal of Computer Industry*, **36**(5), pp. 5-11.

Chen, X. and Rowe, W.B. 1995. Analysis and simulation of the grinding process. *International Journal of Machining Tool Manufacturing*, **36**(8), pp. 883-896.

Choi, S.U. 1995. Enhancing thermal conductivity of fluids with nanoparticles. *Proceeding of the ASME International Mechanical Engineering Congress.*

Demir, H., Gullu, A., Ibrahim, C., and Seker, U. 2010. An investigation into the influences of grain size and grinding parameters on surface roughness and grinding forces when grinding. *Journal of Mechanical Engineering* **7**(8), pp. 447-454.

Ebbrell, S., Wooley, N.H., Tridimas, T.D., Allanson, D.R. and Rowe, W.B. 1999. The effects of cutting fluid application method on the grinding process. *International Journal of Machine Tool and Manufacture*. **40**(2000), pp. 209-223.

Farhat, Z.N. 2003. Wear mechanism of CBN cutting tool during high-speed machining of mold steel. *Journal of Material Science and Engineering*, **61**(5), pp. 101-109.

Hecker, R.L. and Liang, S.Y. 2003. Predictive modelling of surface roughness in grinding. *International Journal of Machine Tools and Manufacturing*, **43**(2003), pp. 755-761.

Hryniewicz, P., Szeril, A.Z. and Jahanmir, S. 1998. Coolant flow in surface grinding with non-porous wheels. *International Journal of Mechanical Science*, **42**(2000), pp. 2347-2367.

Kamely, M.A., Kamil, S.M. and Chong, C.W. 2011. Mathematical modelling of surface roughness in surface grinding operation. *World Academy of Science and Engineering*, pp. 1048-1051.

Kalpakjian, S. and Schmid, S., 2006. *Manufacturing Engineering and Technology*. 5th ed. Pearson, 967 pp.

Krajnik, P., Kopac, J. and Sluga, A. 2005. Design of grinding factor based on response surface methodology. *Journal of Material Technology*, **163**(2005), pp. 629-636.

Krishna, J., Reddy, S. and Reddy, V.K. 2004. Modelling of machining parameters in CNC end milling using pricipal component analysis based neural networks. *Innovative System Design and Engineering*, **2**(3), pp. 223-234.

Ling, Y., 2001. Low-Damage Grinding or Polishing of Silicon Carbide Surface. *Journal of Precision Machining*, **3**(1), pp. 1-8.

Madl, J. 2009. Design of machining. *Journal of Manufacturing Technology*, **9**(4), pp. 81-86.

Madl, J., Jersak, J. and Holesovsky, F. 2003. Quality of machining. *Journal of Manufacturing Technology*, pp. 12-14.

Malkin, S. and Gou, H. 2007. Theory and application of machining with abrasives. *Journal Grinding Technology*, pp.43-49.

Marinescu, I.D., Hitchiner, M., Uhlmann, E., Rowe, W.B., and Inasaki, I. 2007: *Handbook of Machining with Grinding Wheels*. New York: CRC Press, pp. 629.

Midha, P.S., Zhu, C.B. and Trmal, G.J. 1991. Optimum selection of grinding parameter using process modelling and knowledge based system approach. *Journal of Processing Technology*, **28**(3), pp. 189-198.

Oliveira, J.F.G., Silva, E.J., Guo, C. and Hashimoto, F. 2009. Industrial challenges in grinding. *Journal of Manufacturing Technology*, **58**(2), pp. 663-680.

Outwater, J.O. and Shaw, M.C. 1952. Surface temperature in grinding. *Trans of ASME*, **74**(4), pp. 73-86.

Pahlitzsch, G. and Appun, J. 1954. Internal diamond revolution. *Journal of Creative Manufacturing*, pp. 566-569.

Pak, B.C. & Cho, Y.I. 1998. Hydrodynamic and heat transfer study of dispersed fluids with submicron metallic oxide particles. *Experimental Heat Transfer*. **11**(2), pp. 151-170.

Pande, S.J., Halder, S.N., and Lal, G.K. 1979. Evaluation of grinding wheel performance. *Department of Mechanical Engineering*, **58**(1980), pp. 337-248.

Pande, S.J. and Lal, G.K. 1975. Wheel wear in dry surface grinding. *International Journal of Machine Tool Dressing Research*, **16**(4), pp. 179-186.

Pang, J.Z., Wang, M.J. and Duan, C.Z. 2001. White layer and surface roughness in high speed milling of P20 steel. *Journal of Precision and Non-Traditional Machining Technology*, pp. 212-234.

Prabhu, S., and Vinayagam, B.K. 2011. AFM investigation in grinding process with nanofluids using Taguchi analysis. Journal of Advance Manufacturing and Technology, **4**(7), pp. 93-105.

Saidur, R., Leong, K.Y. and Mahammad, H.A. 2010. A review on applications and challenges of nanofluids. *Journal of Renewable and Sustainable Energy*, **15**(4), pp. 1646-1668.

Samek, D., Bilek, O. and Cerny, J. 2011. Prediction of grinding parameter for plastic by Artificial Neural Networks. *International Journal of Mechanics*, **3**(5), pp. 250-261.

Sedlacek, M., Podgornik, B. and Vizintin, J. 2008. Infuence of surface preparation on roughness parameter. *Journal of Wear*, **266**(45), pp. 482-487.

Serrano, E., Rus, G., and Mart ńez, J.G. 2009. Nanotechnology for sustainable energy. *Renew Sust Energy*, **13**(9), pp. 2373–2384.

Shaji, S. and Radhakrishnan, V. 2002. Analysis of process parameter in surface grinding with graphite as lubricant based on the Taguchi Method. *Journal of Materials Processing Technology*, **141**(2003), pp. 51-59.

Shen, B., Shih, A.J. and Tung, S.C. 2008. Appication of Nanofluid in Minimum Quantity Lubricant Grinding. *Society of tribologist and lubricant engineers*, **51**(5), pp. 737-737.

Silva, L.R., Bianchi,E.C., Catai,R.E., Fusse, R.Y., Franc T.V., and Aguiar, P.R. 2005. Study on the behavior of the minimum quantity lubricant- MQL technique under different lubrication and cooling conditions when grinding ABNT 4340 steel. *J. Braz. Soc. Mech. Sci. Eng. XXVII*, pp. 192–199.

Tawakoli, T., Hadad, M., Sadeghi, M.H., and Danehi, A. 2011. Minimum Quantity Lubrication in grinding: effects of abrasive and coolant-lubricant types. *Journal of Cleaner Production*, 19(2011), pp. 2088-2099.

Torrance, A.A. and Badger, J.A. 2000. The relation between the traverse dressing of vitrified grinding wheels and their performance. *Intl. J of Machine Tool Manufacture Design and Research.* **40**(2000), pp. 1787-1811.

Uslu, I., Comert, H., Ipek, M., Celebi. F.G., Ozdemir, O. and Bindal, C. 2006. A comparison of borides formed on AISI 1040 and AISI P20 steel. *Journal of Material and Design*, **28**(2), pp. 1819-1826.

Vickerstaff, T.J. 1975. The influence of wheel dressing on the surface generated in the grinding process. *Intl. J. Mach Tool*, **16,** pp. 145-152.

Webster, J.A., Cui, C. and Mindek, R.B. 1995. Grinding fluid application system design. *Centre for Research and Development University of Connecticut*, **44**(1), pp. 333-338.

Wieczorowski, K., Legutko, S. and Kedzierski, T. 2006. Investigation of the influence of grinding parameters on the errors and surface roughness of holes. *Scientific Bulletin of the Petru Maior University of Targu Mures*, **2**(19), pp. 31-38.

Xie, G.Z. and Huang, H. 2008. An experimental investigation of temperature in high speed deep grinding of partially stabilized Zirconia. *Journal of Machine Tool and Manufacture*, **48**(4), pp. 1562-1568.

Xu, X.P., Yu, T.Q., and Xu, H.J. 2002. Effect of grinding temperatures on the surface intergrity of a Nickel-based superalloy. *Journal of Materials Processing Technology*, **129**, pp. 359-363.

Yan, Y., Zhao, B., and Liu, J. 2009. Ultraprecision surface finishing of nano-ZrO_2 ceramics using two-dimensional ultrasonic assisted grinding. *International Journal of Advance Manufacturing Technology*, **43**(10), pp. 462-467.

Zhong, Z.W. 2003. Grinding of aluminum-based metal matrix composites reinforced with Al_2O_3 or SiC particles. *International Journal of Advance Manufacturing Technology*, **21**(79), pp. 80-85.

Zhou, X., and Xi, F. 2002. Modelling and prediction surface roughness of grinding process. *International Journal of Machine and Manufacture*, **42**(8), pp. 969-977.

APPENDIX A1

DATA COLLECTED FROM THE SINGLE PASS GRINDING EXPERIMENTS USING Al_2O_3 WHEEL WITH CUTTING FLUID OF WATER BASED COOLANT

Table A1: Data collected from the single pass grinding experiments using Al2O3 wheel with cutting fluid of water based coolant

Depth of Cut, µm	Surface Roughness, Ra (µm)			
	1	**2**	**3**	**mean**
5	0.681	0.543	0.642	0.622
7	0.813	0.548	0.775	0.712
9	0.952	0.820	0.817	0.863
11	0.704	0.933	1.093	0.910
13	0.851	1.344	1.144	1.113
15	1.246	1.236	1.436	1.306
17	1.233	1.454	1.480	1.389
19	1.459	1.476	1.538	1.491
21	1.771	1.531	1.759	1.687

APPENDIX A2

DATA COLLECTED FROM THE MULTI PASSES GRINDING EXPERIMENTS USING Al_2O_3 WHEEL WITH CUTTING FLUID OF WATER BASED COOLANT

Table A2: Data collected from the multi passes grinding experiments using Al_2O_3 wheel with cutting fluid of water based coolant

Depth of Cut (µm)	Surface Roughness, Ra (µm)			
	1	2	3	mean
5	0.532	0.467	0.588	0.529
7	0.633	0.498	0.612	0.581
9	0.556	0.672	0.887	0.705
11	0.722	0.887	0.779	0.796
13	0.799	1.121	1.017	0.979
15	1.022	1.098	1.222	1.114
17	1.022	1.308	1.267	1.199
19	1.342	1.126	1.240	1.236
21	1.173	1.255	1.451	1.293

APPENDIX A3

DATA COLLECTED FROM THE SINGLE PASS GRINDING EXPERIMENTS USING SiC WHEEL WITH CUTTING FLUID OF WATER BASED COOLANT

Table A3: Data collected from the single pass grinding experiments using SiC wheel with cutting fluid of water based coolant

Depth of Cut (µm)	Wheel Diameter, D (mm)			Surface Roughness, Ra (µm)			
	Initial	Final	ΔD	1	2	3	mean
5	157.70	157.70	-	0.876	0.711	0.543	0.710
7	155.50	155.50	-	0.882	0.638	0.646	0.722
9	155.38	155.38	-	1.114	0.554	0.831	0.833
11	155.18	155.16	0.02	1.179	0.681	1.092	0.984
13	154.97	154.95	0.02	1.243	0.745	1.192	1.060
15	154.88	154.84	0.04	1.134	1.323	1.671	1.376
17	154.82	154.76	0.06	1.614	1.437	1.725	1.592
19	154.71	154.65	0.06	1.602	1.722	1.704	1.676
21	154.61	154.53	0.08	1.825	1.726	1.693	1.748

APPENDIX A4

DATA COLLECTED FROM THE MULTI PASSES GRINDING EXPERIMENTS USING SiC WHEEL WITH CUTTING FLUID OF WATER BASED COOLANT

Table A4: Data collected from the multi passes grinding experiments using SiC wheel with cutting fluid of water based coolant

Depth of Cut (µm)	Wheel Diameter, D (mm)			Surface Roughness, Ra (µm)			
	Initial	Final	ΔD	1	2	3	mean
5	203.48	203.48	-	0.330	0.916	0.464	0.570
7	203.48	203.48	-	0.428	0.704	0.752	0.628
9	203.48	203.46	0.02	0.542	0.706	0.828	0.692
11	203.46	203.44	0.02	0.751	0.731	0.981	0.821
13	203.44	203.40	0.04	0.930	0.926	0.973	0.943
15	202.54	202.48	0.06	1.073	0.889	1.494	1.152
17	202.48	202.40	0.08	1.013	1.135	1.521	1.223
19	202.40	202.31	0.09	1.123	1.458	1.553	1.378
21	202.31	202.21	0.10	1.146	1.584	1.506	1.412

APPENDIX A5

DATA COLLECTED FROM THE SINGLE PASS GRINDING EXPERIMENTS USING SiC WHEEL WITH CUTTING FLUID OF TiO_2 NANOFLUID

Table A5: Data collected from the single pass grinding experiments using SiC wheel with cutting fluid of TiO_2 nanofluid

Depth of Cut (μm)	Wheel Diameter, D (mm)			Surface Roughness, Ra (μm)			
	Initial	Final	ΔD	1	2	3	mean
5	164.96	164.96	-	0.489	0.501	0.597	0.529
7	164.87	164.87	-	0.512	0.523	0.576	0.537
9	164.78	164.78	-	0.617	0.557	0.521	0.565
11	164.68	164.68	-	0.673	0.746	0.585	0.668
13	164.61	164.61	-	0.718	0.842	0.702	0.754
15	164.52	164.52	-	1.012	0.891	0.785	0.896
17	164.43	164.43	-	0.968	1.134	1.393	1.165
19	164.31	164.31	-	1.102	1.225	1.312	1.213
21	164.24	164.24	-	1.487	1.294	1.152	1.311

APPENDIX A6

DATA COLLECTED FROM THE MULTI PASSES GRINDING EXPERIMENTS USING SiC WHEEL WITH CUTTING FLUID OF TiO_2 NANOFLUID

Table A6: Data collected from the multi passes grinding experiments using SiC wheel with cutting fluid of TiO_2 nanofluid

Depth of Cut (µm)	Wheel Diameter, D (mm)			Surface Roughness, Ra (µm)			
	Initial	Final	ΔD	1	2	3	mean
5	164.20	164.20	-	0.421	0.332	0.312	**0.355**
7	164.11	164.11	-	0.375	0.413	0.349	**0.379**
9	164.02	164.02	-	0.557	0.401	0.365	**0.441**
11	163.89	163.89	-	0.594	0.427	0.548	**0.523**
13	163.80	163.80	-	0.639	0.599	0.778	**0.672**
15	163.71	163.71	-	0.812	0.672	0.619	**0.701**
17	163.63	163.63	-	0.968	0.832	0.897	**0.899**
19	163.54	163.54	-	1.002	0.917	0.904	**0.941**
21	163.47	163.47	-	1.125	1.055	1.096	**1.092**

APPENDIX B1

SEM MICROGRAPH OF SPECIMEN: SiC GRINDING WHEEL-WATER BASED COOLANT-4 PASSES-DOC 5 µm

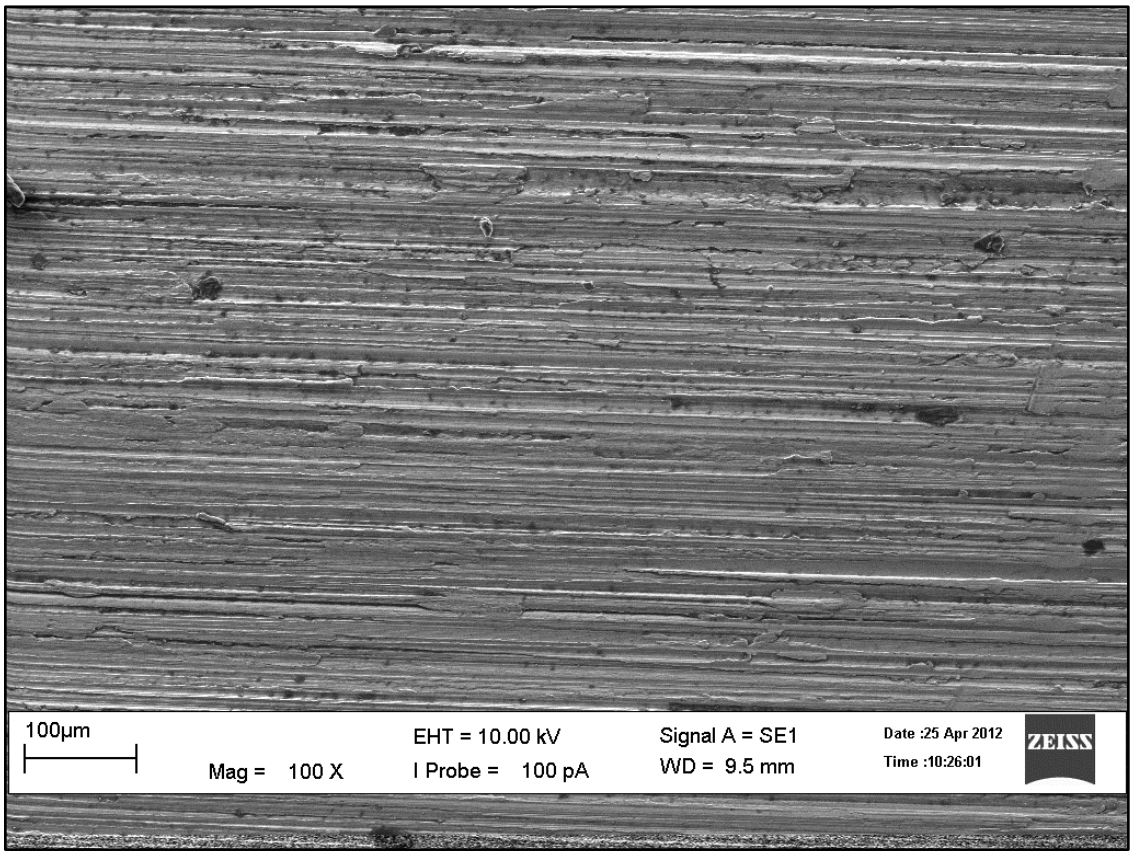

Figure B1: SEM micrograph of grounded surface of specimen: SiC grinding wheel-water based coolant-4 passes-DOC 5 µm. 100x magnification

APPENDIX B2

SEM MICROGRAPH OF SPECIMEN: SiC GRINDING WHEEL-WATER BASED COOLANT-4 PASSES-DOC 11 µm

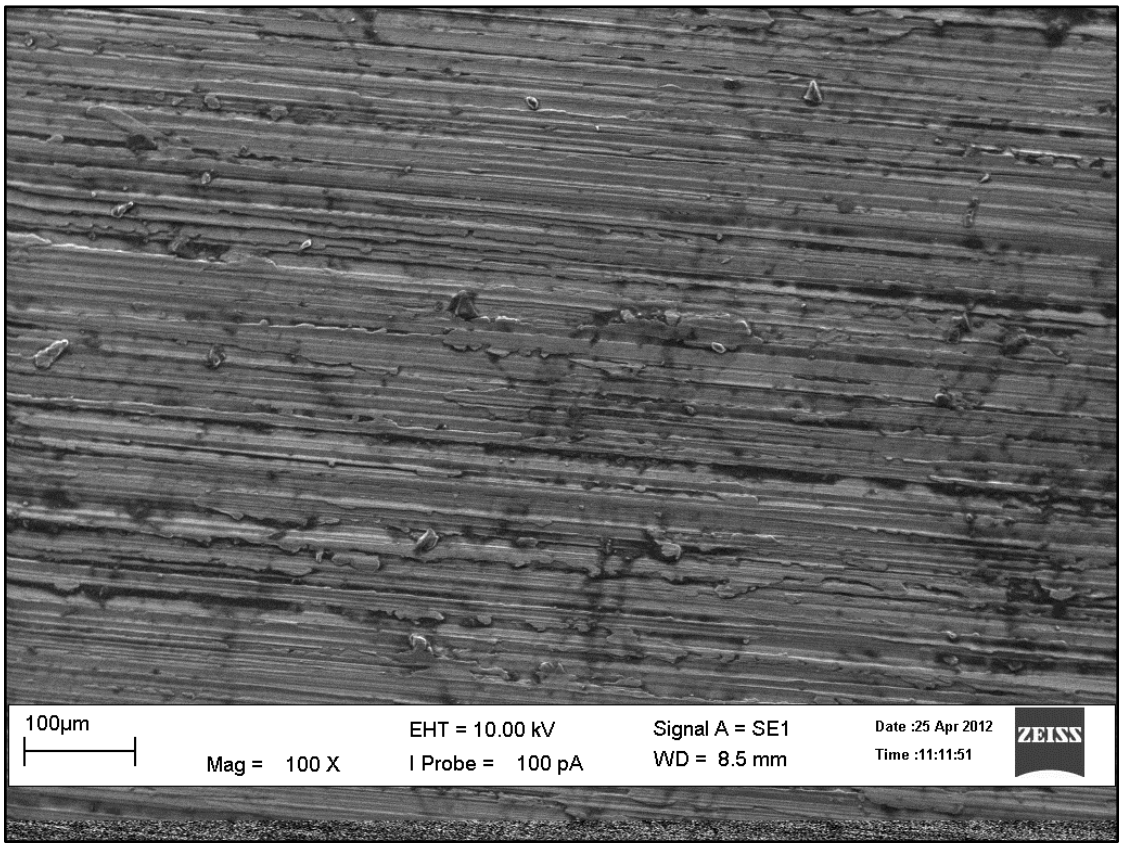

Figure B2: SEM micrograph of grounded surface of specimen: SiC grinding wheel-water based coolant-4 passes-DOC 11 µm. 100x magnification

APPENDIX B3

SEM MICROGRAPH OF SPECIMEN: SiC GRINDING WHEEL-WATER BASED COOLANT-4 PASSES-DOC 21 µm

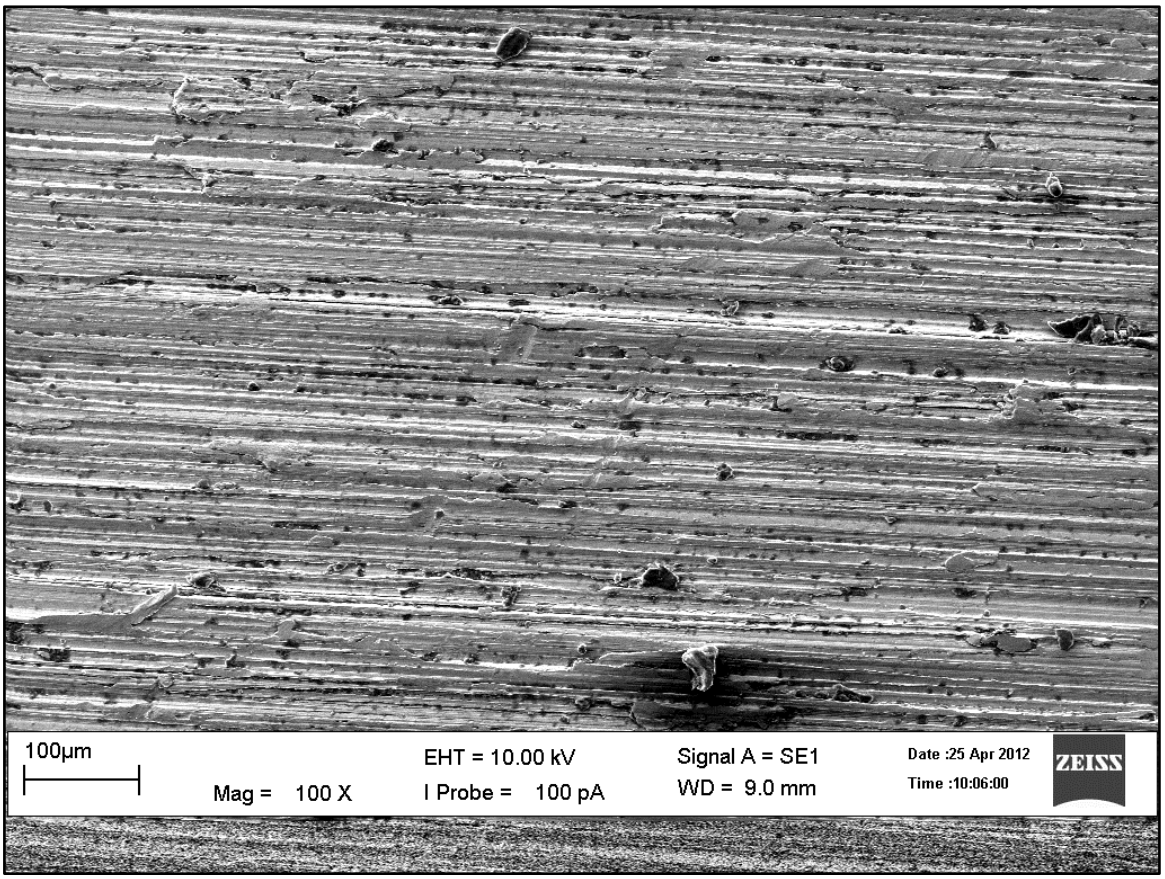

Figure B3: SEM micrograph of grounded surface of specimen: SiC grinding wheel-water based coolant-4 passes-DOC 21 µm. 100x magnification

APPENDIX B4

SEM MICROGRAPH OF SPECIMEN: SiC GRINDING WHEEL-TiO_2 NANOFLUID-4 PASSES-DOC 5 µm

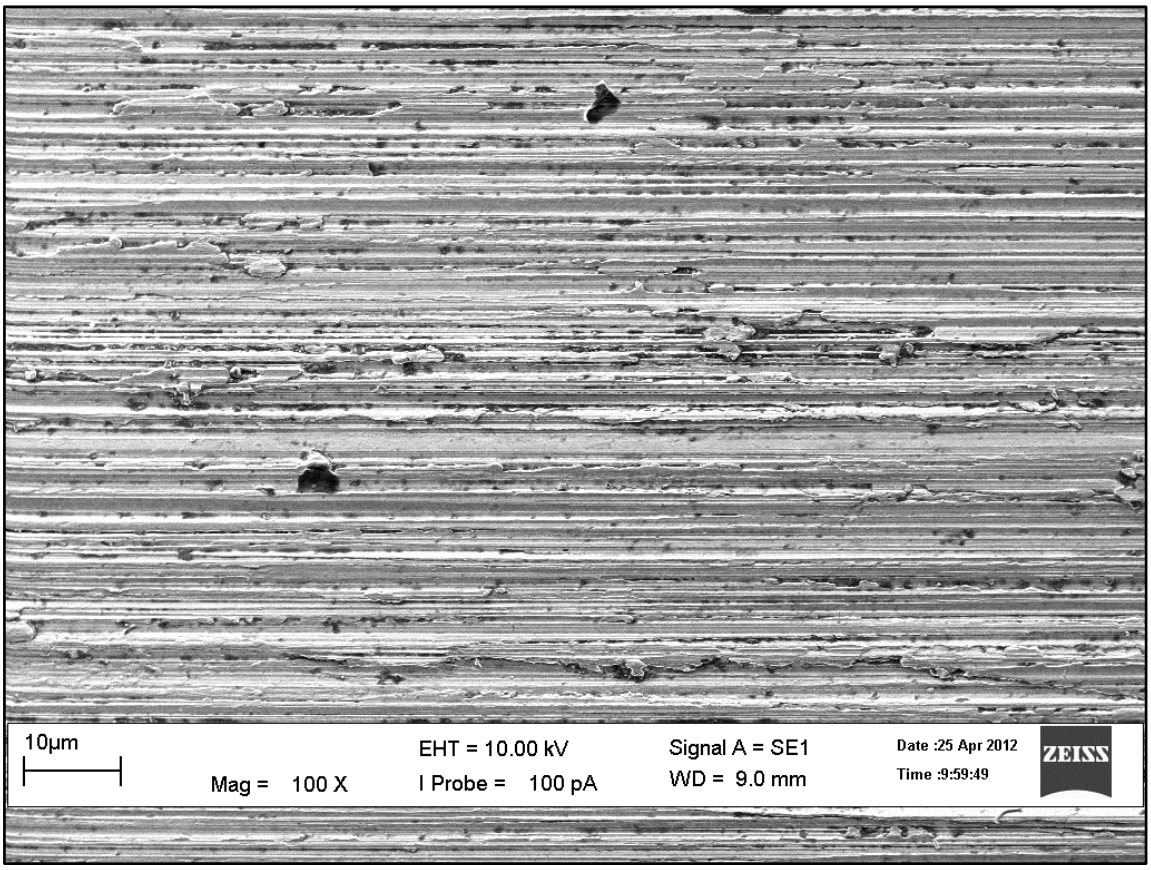

Figure B4: SEM micrograph of grounded surface of specimen: SiC grinding wheel-TiO_2 nanofluid-4 passes-DOC 5 µm. 100x magnification

APPENDIX B5

SEM MICROGRAPH OF SPECIMEN: SiC GRINDING WHEEL-TiO_2 NANOFLUID-4 PASSES-DOC 11 µm

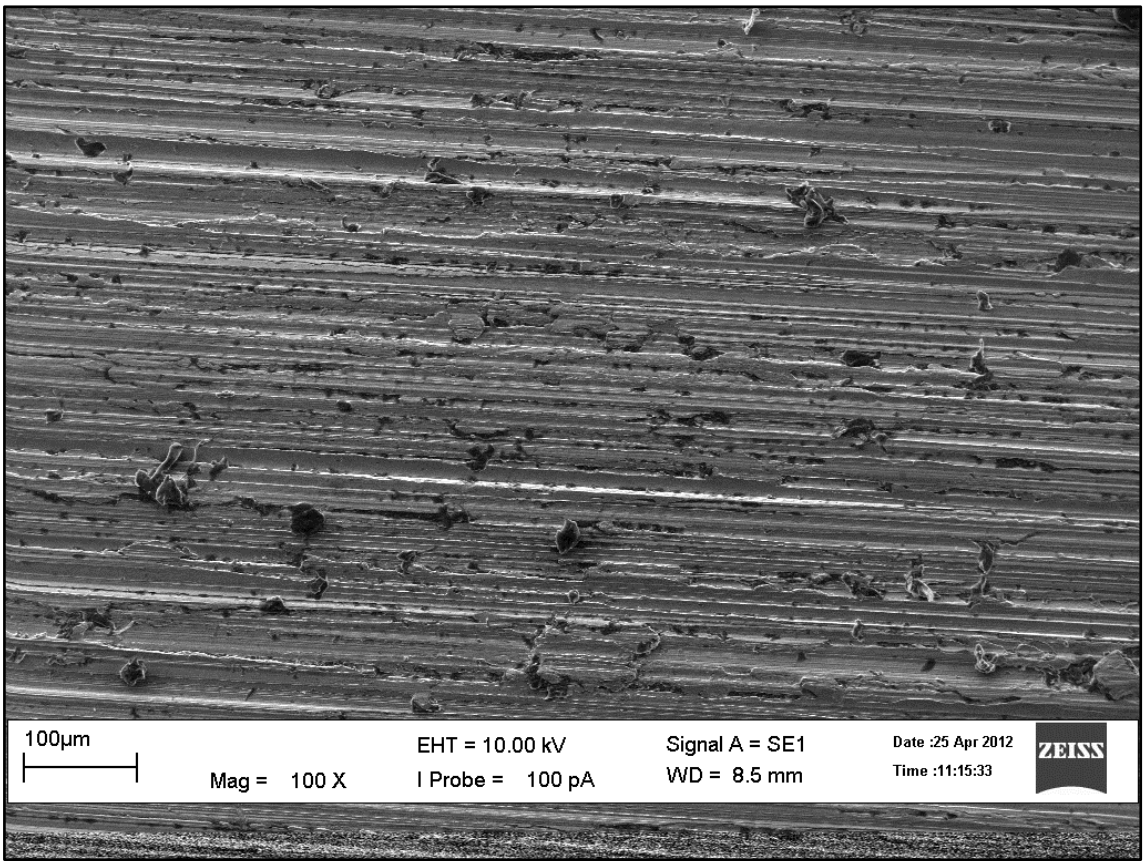

Figure B5: SEM micrograph of grounded surface of specimen: SiC grinding wheel-TiO_2 nanofluid-4 passes-DOC 11 µm. 100x magnification

APPENDIX B6

SEM MICROGRAPH OF SPECIMEN: SiC GRINDING WHEEL-TiO_2 NANOFLUID-4 PASSES-DOC 21 µm

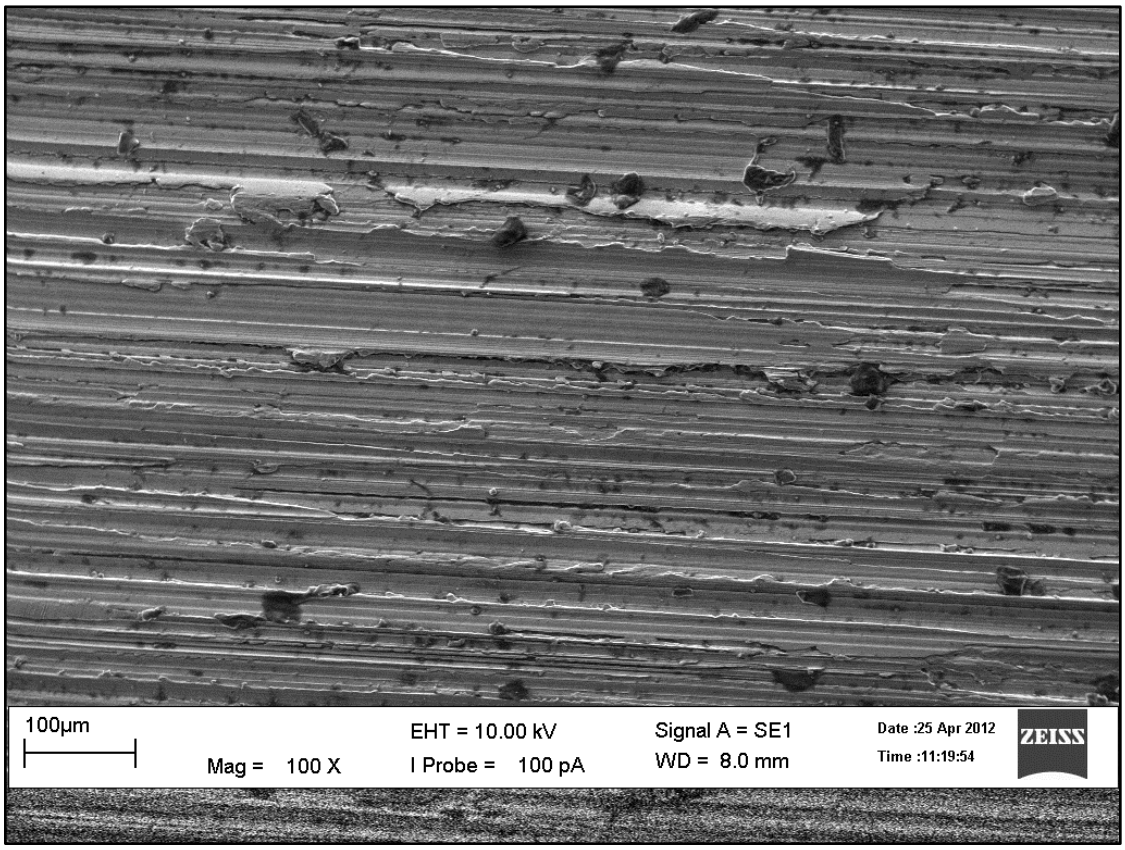

Figure B6: SEM micrograph of grounded surface of specimen: SiC grinding wheel-TiO_2 nanofluid-4 passes-DOC 21 µm. 100x magnification

APPENDIX C1

RESULT OF THE ANN PREDICTION MODELS FOR SINGLE PASS GRINDING EXPERIMENTS USING Al_2O_3 WHEEL WITH CUTTING FLUID OF WATER BASED COOLANT

Table C1: Result of the ANN prediction modelling for single pass grinding experiments using Al_2O_3 wheel with cutting fluid of water based coolant

Depth of Cut	Exp. result	ANN modelling result
5	0.622	0.701966
7	0.712	0.730976
9	0.863	0.791706
11	0.91	0.914184
13	1.113	1.113
15	1.306	1.324652
17	1.389	1.469106
19	1.491	1.545132
21	1.687	1.58252
23	-	1.601319
25	-	1.611172
27	-	1.616523
29	-	1.619505
31	-	1.621197
33	-	1.622168
35	-	1.62273
37	-	1.623057
39	-	1.623249
41	-	1.623362
43	-	1.623428
45	-	1.623468
47	-	1.623491
49	-	1.623505
51	-	1.623513

APPENDIX C2

RESULT OF THE ANN PREDICTION MODELS FOR MULTI PASSES GRINDING EXPERIMENTS USING Al_2O_3 WHEEL WITH CUTTING FLUID OF WATER BASED COOLANT

Table C2: Result of the ANN prediction modelling for multi passes grinding experiments using Al_2O_3 wheel with cutting fluid of water based coolant

Depth of Cut	Exp. result	ANN modelling result
5	0.529	0.61544
7	0.581	0.645099
9	0.705	0.704999
11	0.796	0.815203
13	0.979	0.967467
15	1.114	1.101781
17	1.199	1.181277
19	1.236	1.220056
21	1.293	1.238432
23	-	1.247443
25	-	1.252046
27	-	1.25447
29	-	1.255773
31	-	1.25648
33	-	1.256867
35	-	1.25708
37	-	1.257197
39	-	1.257262
41	-	1.257297
43	-	1.257317
45	-	1.257328
47	-	1.257334
49	-	1.257337
51	-	1.257339

APPENDIX C3

RESULT OF THE ANN PREDICTION MODELS FOR SINGLE PASS GRINDING EXPERIMENTS USING SiC WHEEL WITH CUTTING FLUID OF WATER BASED COOLANT

Table C3: Result of the ANN prediction modelling for single pass grinding experiments using SiC wheel with cutting fluid of water based coolant

Depth of Cut	Exp. result	ANN modelling result
5	0.71	0.75752
7	0.722	0.78412
9	0.833	0.840582
11	0.984	0.955735
13	1.06	1.154231
15	1.376	1.396925
17	1.592	1.583039
19	1.676	1.677146
21	1.748	1.715135
23	-	1.729904
25	-	1.736033
27	-	1.738818
29	-	1.740187
31	-	1.740897
33	-	1.741279
35	-	1.741489
37	-	1.741606
39	-	1.741671
41	-	1.741708
43	-	1.741728
45	-	1.74174
47	-	1.741747
49	-	1.741751
51	-	1.741753

APPENDIX C4

RESULT OF THE ANN PREDICTION MODELS FOR MULTI PASSES GRINDING EXPERIMENTS USING SiC WHEEL WITH CUTTING FLUID OF WATER BASED COOLANT

Table C4: Result of the ANN prediction modelling for multi passes grinding experiments using SiC wheel with cutting fluid of water based coolant

Depth of Cut	Exp. result	ANN modelling result
5	0.57	0.642213
7	0.628	0.666922
9	0.692	0.718477
11	0.821	0.820998
13	0.943	0.982025
15	1.152	1.145041
17	1.223	1.251061
19	1.378	1.305155
21	1.412	1.331299
23	-	1.34427
25	-	1.350969
27	-	1.354542
29	-	1.356492
31	-	1.357573
33	-	1.358178
35	-	1.358519
37	-	1.358712
39	-	1.358823
41	-	1.358886
43	-	1.358922
45	-	1.358943
47	-	1.358955
49	-	1.358962
51	-	1.358966

APPENDIX C5

RESULT OF THE ANN PREDICTION MODELS FOR SINGLE PASS GRINDING EXPERIMENTS USING SiC WHEEL WITH CUTTING FLUID OF TiO_2 NANOFLUID

Table C5: Result of the ANN prediction modelling for single pass grinding experiments using SiC wheel with cutting fluid of TiO_2 nanofluid

Depth of Cut	Exp. result	ANN modelling result
5	0.529	0.553022
7	0.537	0.560127
9	0.565	0.576326
11	0.668	0.617125
13	0.754	0.722147
15	0.896	0.92904
17	1.165	1.137645
19	1.213	1.241155
21	1.311	1.278287
23	-	1.291737
25	-	1.297217
27	-	1.299713
29	-	1.300944
31	-	1.301581
33	-	1.30192
35	-	1.302105
37	-	1.302205
39	-	1.302261
41	-	1.302292
43	-	1.302308
45	-	1.302318
47	-	1.302323
49	-	1.302326
51	-	1.302328

APPENDIX C6

RESULT OF THE ANN PREDICTION MODELS FOR MULTI PASSES GRINDING EXPERIMENTS USING SiC WHEEL WITH CUTTING FLUID OF TiO_2 NANOFLUID

Table C6: Result of the ANN prediction modelling for multi pasess grinding experiments using SiC wheel with cutting fluid of TiO_2 nanofluid.

Depth of Cut	Exp. result	ANN modelling result
5	0.355	0.420882
7	0.379	0.436256
9	0.441	0.465788
11	0.523	0.522999
13	0.672	0.622566
15	0.701	0.752092
17	0.899	0.864704
19	0.941	0.935748
21	1.092	0.974683
23	-	0.995724
25	-	1.007501
27	-	1.01438
29	-	1.01855
31	-	1.02115
33	-	1.022807
35	-	1.02388
37	-	1.024582
39	-	1.025046
41	-	1.025355
43	-	1.025561
45	-	1.025699
47	-	1.025792
49	-	1.025855
51	-	1.025897

APPENDIX D1

GANTT CHART PSM 1

No	Project Activities	Weeks (Semester 1)														
		1	2	3	4	5	6	7	8	9	10	11	12	13	14	15
1	Discuss on the title of PSM 1															
2	Discuss the objective and scopes															
3	Literature study and find the related info															
4	Discuss on the methodology and experiment set up															
5	Grinding training															
6	Grinding Experiment with water based coolant															
7	Finalize Chapter 1, 2 and 3															
8	Report submission															
9	Presentation															

Planning	
Actual Schedule	

APPENDIX D2

GANTT CHART PSM 2

No	Project Activities	Weeks (Semester 2)													
		1	2	3	4	5	6	7	8	9	10	11	12	13	14
1	Nanofluid preparation														
2	Nanofluid observation														
3	Grinding experiment with TiO_2 nanofluid														
4	Validation of experimental data														
5	Compute ANN prediction models														
6	Metallographic analysis														
7	Thesis writing														
8	Presentation														

Planning	
Actual Schedule	